DOI: 10.1590/2317-4889201620150059

ARTICLE

Stable (C, O, S) isotopes and whole-rock geochemistry of carbonatites from Alto Paranaíba Igneous Province, SE Brazil

Isótopos estáveis (C, O, S) e geoquímica de rocha total de carbonatitos da Província Ígnea Alto Paranaíba – SE Brasil

Caroline Siqueira Gomide[1]*, José Affonso Brod[2,3], Lucieth Cruz Vieira[4], Tereza Cristina Junqueira-Brod[2], Ivan Alejandro Petrinovic[5], Roberto Ventura Santos[4,6], Elisa Soares Rocha Barbosa[2], Luis Henrique Mancini[6]

ABSTRACT: The present work investigates the relationship between whole-rock geochemistry and stable isotope composition from carbonatites belonging to the Tapira, Araxá, Salitre, Serra Negra, Catalão I, and Catalão II alkaline-carbonatite complexes of the Alto Paranaiba Igneous Province (APIP), central Brazil and from the Jacupiranga Complex, of the Ponta Grossa Province, southeast Brazil. The APIP complexes are ultrapotassic, comprising bebedourites, phoscorites, nelsonites, and carbonatites, whereas Jacupiranga is a sodic complex composed of ijolite-series rocks, syenites, carbonatites, and alkaline gabbros. The geochemistry data allied to mineralogical constraints allowed us to classify the carbonatites into five groups, and to devise a chemical index (BaO/(BaO+SrO)) to gauge the magmatic evolution of the studied carbonatites.The APIP carbonatites evolve from apatite-rich calciocarbonatites toward Ba-, Sr-, and rare earth element (REE)-rich magnesiocarbonatites. This evolution is mostly driven by apatite, phlogopite, dolomite, and calcite fractionation and consequent enrichment in monazite, norsethite, and strontianite. Stable isotope data show a wide diversity of petrogenetic processes in play at the APIP, relatively to the Jacupiranga Complex, which is interpreted as a result of the shallower intrusion levels of the APIP complexes. Such shallower emplacement, at low lithostatic pressure, allowed for a complex interplay of fractional crystallization, liquid immiscibility, degassing, and interaction with hydrothermal and carbohydrothermal systems.

KEYWORDS: Carbonatite; carbonates; geochemistry; stable isotopes; APIP.

RESUMO: *O presente trabalho investiga a relação entre a geoquímica de rocha total e a composição dos isótopos estáveis de carbonatitos pertencentes aos complexos alcalino-carbonatíticos de Tapira, Araxá, Salitre, Serra Negra, Catalão I e Catalão II da Província Ígneado Alto Paranaiba (APIP) e do Complexo Jacupiranga, da Província Grossa Ponta. Os complexos do Alto Paranaíba são ultrapotássicos, compreendendo bebedouritos, foscoritos, nelsonitos e carbonatitos, enquanto Jacupiranga é um complexo composto por rochas sódicas da série ijolítica, sienitos, carbonatitos e gabros alcalinos. Os dados geoquímicos, aliados a condições mineralógicas, nos permitiram classificar os carbonatitos em 5 grupos, e elaborar um índice químico (BaO/(BaO+SrO)) para avaliar a evolução magmática dos carbonatitos estudados. Os carbonatitos APIP evoluem de calciocarbonatitos ricos em apatita em direção a magnesiocarbonatitos ricos em Ba, Sr e elementos terra raras (ETR). Essa evolução é impulsionada principalmente por fracionamento de apatita, flogopita, dolomita e calcita, e enriquecimento em monazita, norsethita e estroncianita. Dados de isótopos estáveis mostram uma grande diversidade de processos petrogenéticos presentes no Alto Paranaíba, relativamente ao Complexo Jacupiranga, que é interpretado como um resultado dos níveis de intrusão mais rasos dos complexos APIP. Tal colocação, à baixa pressão litostática, permitiu uma interação complexa entre cristalização fracionada, imiscibilidade de líquidos, desgaseificação e interação com sistemas hidrotermais e carbohidrotermais.*

PALAVRAS-CHAVE: *Carbonatito; geoquímica; isótopos estáveis; APIP.*

[1]Faculdade UnB Planaltina, Universidade de Brasília – UnB, Brasília (DF), Brazil. *E-mail: caroline.gomide@gmail.com*

[2]Faculdade de Ciências e Tecnologia, Universidade Federal de Goiás – UFG, Goiânia (GO), Brazil. *E-mail: jabrod@gmail.com, tcjbrod@gmail.com, elisa.barbosa@uol.com.br*

[3]Centro Regional para o Desenvolvimento Tecnológico e Inovação, Universidade Federal de Goiás – UFG, Goiânia (GO), Brazil. *E-mail: jabrod@gmail.com*

[4]Instituto de Geociências, Campus Universitário Darcy Ribeiro, Universidade de Brasília – UnB, Brasília (DF), Brazil. *E-mail: lucieth@gmail.com, rventura@unb.br*

[5]CICTERRA, Facultad de Ciencias Exactas, Físicas y Naturales, Universidad Nacional de Córdoba, Córdoba, Argentina. *E-mail: ipetrinovic@yahoo.com*

[6]Laboratório de Estudos Geodinamicos e Ambientais, Campus Universitário Darcy Ribeiro, Universidade de Brasília – UnB, Brasília (DF), Brazil. *E-mail: lmancini@unb.br*

*Corresponding author.

Manuscript ID: 20150059. **Received in:** 12/17/2015. **Approved in:** 06/05/2016.

INTRODUCTION

Brazilian alkaline provinces have been studied by a range of techniques such as whole-rock geochemistry, mineral chemistry, stable and radiogenic isotope geochemistry, with a range of petrogenetic aplications (Gomide *et al.* 2013, Barbosa 2009, Cordeiro *et al.* 2011, Grasso 2010, Ribeiro 2008, Comin-Chiaramonti *et al.* 2001, 2005, Traversa 2001, Andrade *et al.* 2002, Huang *et al.* 1995, Santos & Clayton 1995, Ulbrich & Gomes 1981). We aim to contribute to the knowledge of carbonatite petrogenetic evolution, investigating the relationships between whole-rock geochemistry and stable isotope geochemistry data, reporting geochemical and isotopic data from carbonatites of the Late-Cretaceous Alto Paranaíba Igneous Province (APIP), and discuss their implications for magma evolution, both at single-complex and Province-wide scales. The results obtained are compared with the Early-Cretaceous Jacupiranga carbonatite complex, in the Ponta Grossa Province.

Alkaline rocks and alkaline-carbonatite associations include highly variable petrographic types and correspondingly extensive nomenclature. We adopt the nomenclature proposed by Le Maitre *et al.* (2002) for carbonatites and rocks of the ijolite series, Sahama (1974) for kamafugites, Yegorov (1993) for phoscorites, and Barbosa *et al.* (2012) for bebedourites.

The APIP alkaline-carbonatite complexes are multistage intrusions formed by rocks derived from the bebedourite, carbonatite, and phoscorite series, which are related to each other by a complex interplay of fractional crystallization, liquid immiscibility, and degassing (Brod *et al.* 2004, Ribeiro 2008, Barbosa 2009, Cordeiro *et al.* 2010, Barbosa *et al.* 2012, Brod *et al.* 2013).

GEOLOGICAL SETTING

The APIP, located in Minas Gerais and Goiás State, is the result of an intense mafic ultramafic alkaline and ultrapossic magmatism (Brod *et al.* 2004) during the Late Cretaceous. The province is composed by large volumes of kamafugites (Mata da Corda Group lavas and pyroclastics, and countless subvolcanic bodies), subordinate kimberlites, rare lamproites, and several alkaline-carbonatite plutonic complexes (Almeida & Svisero 1991, Leonardos *et al.* 1991, Gibson *et al.* 1995, Brod *et al.* 2000, 2004, Comin-Chiaramonti *et al.* 2005, Carlson *et al.* 2007). Figure 1 shows the location of the APIP complexes.

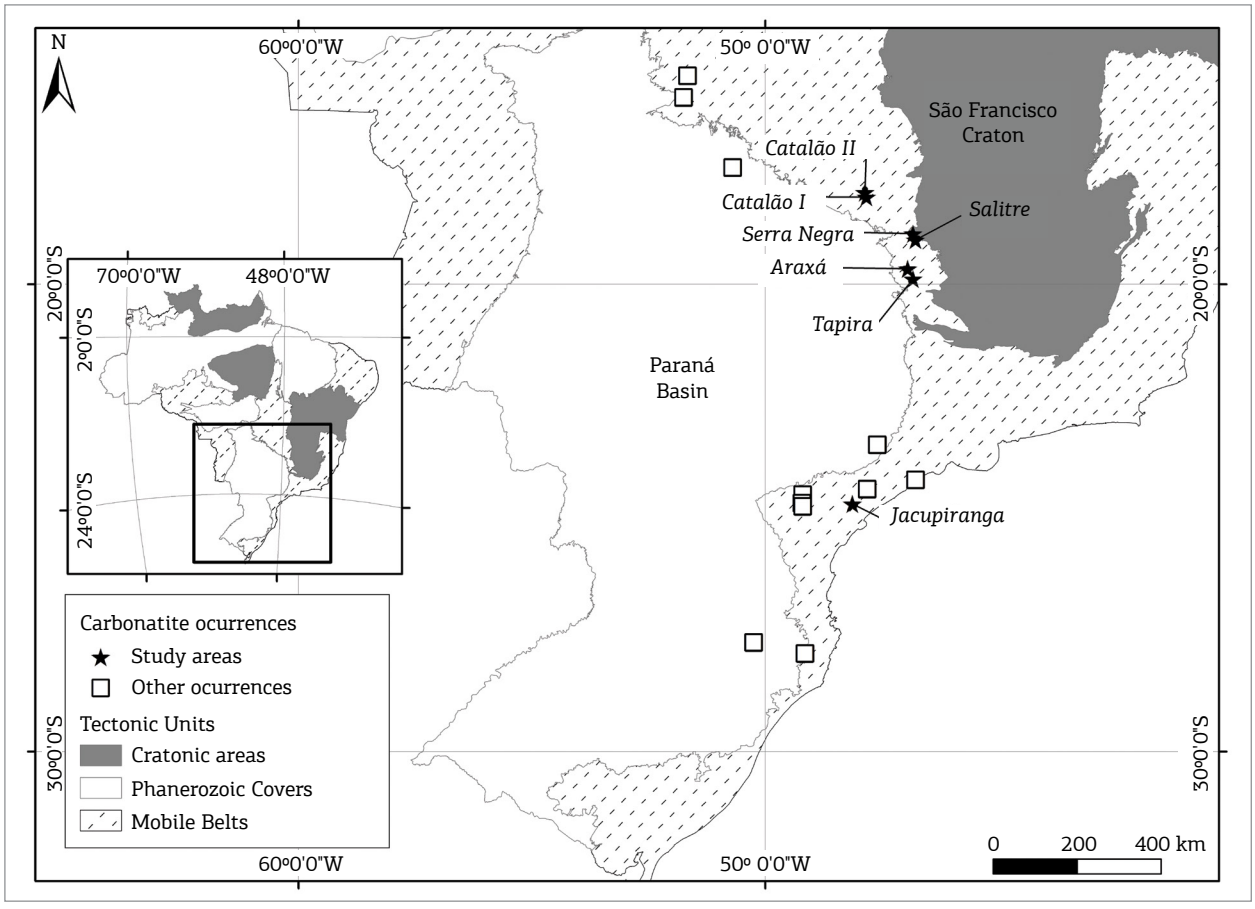

Figure 1. Alkaline-carbonatite complexes northeast and east of the Paraná Basin, modified from Oliveira *et al.* (2004) and Wooley and Kjarsgaard (2008).

Gibson *et al*. (1995, 1997) and Brod *et al*. (2005) correlated the Late-Cretaceous (ca. 85 Ma) magmatism at the northern and northeastern borders of the Paraná Basin with the impact of the Trindade mantle plume (Gibson *et al*. 1995) at the subcontinental lithosphere.

The Province was established along an elongated NW–SE structure called the Alto Paranaíba Arc. The alkaline magmas were emplaced into Precambrian rocks from the internal and external zones of the Brasilia Fold Belt. Kamafugite is by far the dominant rock type in the province, forming one of the few known kamafugite-carbonatite associations (Brod *et al*. 2000).

The ultramafic rocks of all complexes show variable degrees of metasomatism by fluids resulting from carbonatite differentiation. The relatively shallow characteristics of the APIP intrusions are indicated by C and O isotopes (Santos & Clayton 1995), within-magma chamber pyroclastic deposits (Ribeiro *et al*. 2005), similarities between bebedourites and xenoliths in volcanic and subvolcanic kamafugites in the province (Seer & Moraes 1988, Brod *et al*. 2000), and the extent of degassing/metasomatism.

The APIP alkaline-carbonatite complexes comprise, from north to south, Catalão II, Catalão I, Serra Negra, Salitre II, I and III, Araxá, and Tapira; these complexes are ultrapotassic and have a kamafugitic affinity (Lloyd & Bailey 1991, Gibson *et al*. 1995, Brod 1999, Brod *et al*. 2000), forming a carbonatite-kamafugite association compared to that described in Italy (Stoppa & Cundari 1995, Stoppa & Wooley 1997).

The Catalão I Complex is composed of dunite, clinopyroxenite, bebedourite, carbonatite, phoscorite, nelsonite, and phlogopitite, and is evolved from phlogopite-picrite magma by several stages of fractional crystallization and liquid immiscibility. Magnesiocarbonatite is the dominant carbonatite type in the complex (Brod *et al*. 2004, Ribeiro 2008, Cordeiro *et al*. 2010).

Catalão II is composed of pyroxenite, quartz-syenite, alkali-feldspar syenite, calciocarbonatite, silicocarbonatite, lamprophyre, and phlogopitite (Machado Junior 1992). Calciocarbonatites dominate over magnesiocarbonatites. Regarding the phoscorite series, the northern portion of the complex is dominated by phoscorite, whereas the south part is dominated by nelsonite (Palmieri *et al*. 2011).

Serra Negra is the largest APIP carbonatite complex with an area of 65 km^2. It intruded quartzites from the Canastra Group, generating a very pronounced dome structure. The complex is composed by dunites, bebedourites, calciocarbonatites, magnesiocarbonatites, trachytes.

Salitre consists of three bodies located to the south of the Serra Negra Complex. The rocks present in the complex include bebedourites, dunites, perovskitites, tinguaites, trachytes, phoscorites, apatite-carbonatites, calciocarbonatite, magnesiocarbonatites, and fenites (Mariano & Marchetto 1991, Brod *et al*. 2004, Barbosa *et al*. 2009).

The Araxá Complex is composed of carbonatites, phoscorites, and metasomatic phlogopitites derived from ultramafic rocks. Magnesiocarbonatite is the dominant carbonatite type in this complex. The intrusion generated a dome structure in schists and quartzites from the Ibiá Group (Seer 1999).

Tapira is an approximately elliptic complex, composed of bebedourite with subordinate carbonatite and syenite, and rare melilitolite and dunite, all cut by ultramafic dikes of kamafugite affinity. Calciocarbonatite dominates over magnesiocarbonatite (Brod *et al*. 2003).

Jacupiranga, the only complex from the Ponta Grossa Province studied in this work, is located about 10 km west of the city of Jacupiranga, São Paulo State. The complex is composed by pyroxenite (jacupirangite), serpentinized peridotite, ijolite, nepheline-syenite, carbonatite, essexite, monchiquite, and tinguaíte (Gomes *et al*. 1990). It intruded Precambrian metasedimentary rocks of the Açungui Group (Ruberti *et al*. 2005) and has an oval (approximate 65 km^2) shape, with a small-elongated core composed of carbonatite intruding jacupirangites. Gaspar and Wyllie (1982, 1983) identified five successive carbonatite intrusions called C1 to C5, from the oldest to the most recent. C1, C3, and C4 are dominated by calciocarbonatite; C2 is dominated by dolomite calcite carbonatite; and C5 by ankerite carbonatite (Gaspar & Wyllie 1983).

MATERIALS AND METHODS

Analyzed samples were first examined under a petrographic microscope to determine mineralogical and textural characteristics. Selected samples were ground in an agate mill and sent to the ACME Labs for whole-rock chemical analysis (ACME 4A and 4B packages). Powders produced from whole-rock and/or mineral separates were analyzed for C and O isotopes using a Delta V plus gas source mass spectrometer at the University of Brasília. The S isotopes data are from Gomide *et al*. (2013).

RESULTS AND DISCUSSION

The studied APIP carbonatites were classified into five groups on the basis of their modal composition, petrographic characteristics, and interpretations and evolution models from the previous works (Barbosa 2009, Brod 1999, Cordeiro 2009, Cordeiro *et al*. 2010, Cordeiro *et al*. 2011,

Grasso 2010, Palmieri 2011, Ribeiro 2008, Ribeiro *et al.* 2014). The key minerals modal compositions are shown in Figure 2, and the geochemical and textural characteristics, and the evolution stage of each group are summarized in Table 1.

Early-stage carbonatites (C1) are rich in apatite, phlogopite, and magnetite, but all the three phases tend to diminish or disappear at the intermediate stages (C2 or C3) resuming crystallization in later stages (C4 and C5). Barite is typically lacking in the initial stages, appearing for the first time at calciocarbonatites C3 and becoming more abundant toward later stages.

Monazite is restricted to the most evolved carbonatites. Calcite is the dominant carbonate phase at C1 and C3, while dolomite dominates in C2, C4, and C5 groups. Strontianite and norsethite appear initially as liquidus phases in calciocarbonatite C3 and increase in abundance toward more evolved carbonatites. Barytocalcite is present in C3, but only locally, and restricted to this group.

WHOLE-ROCK GEOCHEMISTRY

Whole-rock chemistry data were plotted in the carbonatite classification diagram of Woolley and Kempe (1989). Carbonatites from groups C1 and C3 are plotted in the field of calciocarbonatite, whereas carbonatites from groups C2, C4, and C5 are plotted in the field of magnesiocarbonatites (Fig. 3).

The C1-type calciocarbonatites (Fig. 3) are present in Catalão II, Salitre, Tapira, and Jacupiranga. Mineralogically, they are unevolved, containing large amounts of silicates such as olivine, amphibole and Al-rich phlogopite, carbonate minerals restricted to calcite and possibly dolomite, and significant amounts of apatite and magnetite.

The C3 calciocarbonatites (Fig. 3) were identified only in samples from Tapira and differ from the C1 calciocarbonatites because they contain primary norsethite, baritocalcite, and tetraferriphlogopite instead of aluminous phlogopite, indicating that C3 are a more evolved version of calciocarbonatite. The presence of Sr-, Ba-, and rare earth element (REE)-rich exsolutions in calcite suggests crystallization of the latter at relatively high temperature. Similar characteristics were observed by Brod (1999) for Tapira carbonatites and by Cordeiro *et al.* (2011) for Catalão I.

The C2-type magnesiocarbonatites (Fig. 3) are present in Catalão I, Serra Negra, Salitre, and Jacupiranga. These rocks have a simple primary carbonate composition, restricted to dolomite and calcite. The presence of abundant exsolutions indicates that these carbonates crystallized at relatively high temperature. This group of magnesiocarbonatites is little differentiated, but may not represent the most primitive magnesiocarbonatite in the province, since magnesiocarbonatites with olivine are described in Salitre and Serra Negra (Barbosa 2009, Grasso 2010).

The C4 group consists of Ba- and REE-rich magnesiocarbonatites (Fig. 3), whose carbonate assembly consists mainly of dolomite, Fe-dolomite, and strontianite (often colomorph). This group comprises samples from Araxá, Tapira, and Salitre.

The C5-type magnesiocarbonatites studied in this work are present in Catalão I, Catalão II, Araxá, and Tapira. They are enriched in Ba and characterized by a wide variety of carbonates, including dolomite, Fe-dolomite, norsethite, burbankite, calcite, and strontianite.

The determination of the evolution stage in carbonatites is a difficult task, because the concentration of elements typically used to monitor differentiation in common magmas may be strongly modified by the crystallization of specific phases in carbonatite magmas. For example, MgO is an essential constituent of olivine, which is an early-stage phase in the carbonatite magma, but also in dolomite, which may be a late-stage mineral. The same reasoning applies to FeO (early-stage magnetite and late-stage Fe-carbonates). SiO_2 and Al_2O_3 essentially participate

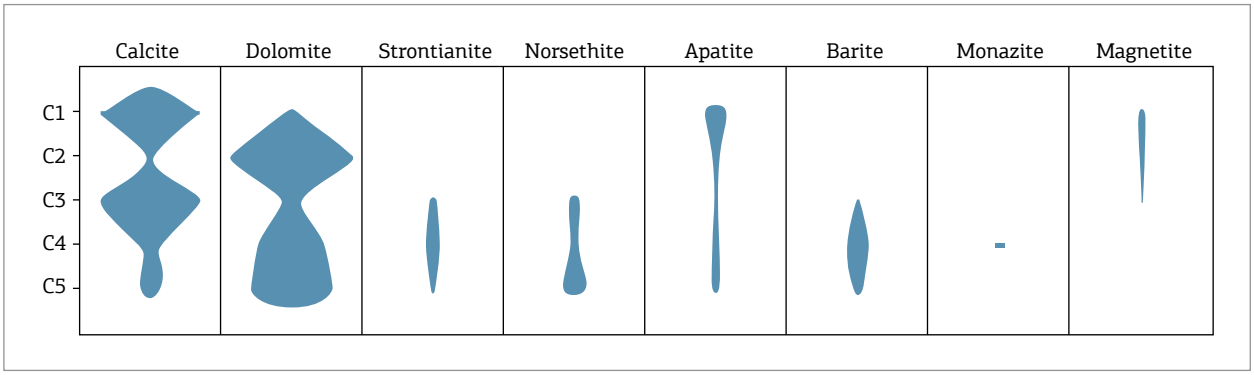

Figure 2. Comparative modal composition of key mineral phases with different carbonatite evolution stages.

Table 1. Characterization of the studied carbonatite groups based on mineralogy, textures, chemistry and evolution stage. Jacupiranga samples are taken as representative of the least evolved stages.

	Subgroups	Complex	Mineralogy	Geochemistry characteristics	Carbonates	Grain Size
C1	C1a	Jacupiranga	cb, ap, ol,± po, ± py, ± mag, ± ilm	Ca-cbt com P_2O_5 > 9%	Cal >> Dol	coarser
	C1b	Jacupiranga	cb, ap, po, ± phl, ± pn,	Ca-cbt com P_2O_5 < 9%	Cal >> Dol	
	C1a	Salitre, Tapira	cb, ap, phl, tfp, po, ±py, ±pcl, ± prv, ±mag, ±ilm, ± ccp, ±ol	Ca-cbt with P_2O_5 > 3%	Cal >> Dol	
	C1b	Catalão II, Salitre, Tapira	cb, ap, phl, tfp, mag, po, py, ± amp, ±pcl, ± brt, ± ccp, ± ol ± mrc	Ca-cbt with P_2O_5 < 3%	Cal >> Dol	
C2		Catalão I, Serra Negra, Salitre	cb, phl, tfp, mag, py, ± ap, ± brt, ±pcl, ± ccp, ± po,± ilm, ± ol	Mg-cbt	Dol > Cal	
C3		Tapira Araxá	cb, tfp, brt, py, ± ccp, ± po, ± ap, ± ol, ± mag, ± ilm	Ca-Cbt	cal, bacc, nor, str	
C4		Araxá, Catalão I, Catalão II, Tapira, Salitre	cb, cb coloidal, brt, py, mnz, ±phl, ±tfp, ±mag, ±pcl,±ap,±ccp ±po	Ba-mg-cbt com ETR	dol, fe-dol, str, anc, par, bast	
C5	C5a	Catalão I, Catalão II, Araxá, Tapira	cbt, brt, phl, tfp, ap, py, ±mag, ±ilm, ±pcl ,±ccp, ±po, ±mnz	Ba-Mg-cbt	Dol and fe-dol > cal; nor, bkt, str	
	C5b	Catalão I, Salitre	cbt, ap, brt, py, ±mag, ±ilm, ±mnz	Ba-Mg-cbt	Dol > cal	

Amp: amphibole, Ap: apatite, Brt: barite, Cal: calcite, Cb: carbonate, Ccp: chalcopyrite, Dol: dolomite, Ilm: ilmenite, Mag: magnetita, Mnz: monazite, Mrc: marcasite, Ol: olivine, Pcl: pyrochlore, Phl: phlogopite, Pn: pentlandite, Po: pyrrhotite, Prv: perovskite, Py: pyrite, Str: strontianite (Whitney & Evans 2010). Anc: ancyllite, Bacc: barytocalcite, Bast: bastnaesite, Bkt: burbankite, Nor: norsethite, Par: parisite, Tfp: tetraferriphlogopite.

in silicates and should decrease with the evolution of carbonatite magma, as silicates are mostly crystallized at the early stages. However, the concentration of these elements is generally very low in carbonatites and their use as a differentiation index is limited for the most part of the evolution range.

There is a literature consensus (e.g. Buhn & Rankin 1999, Chakhmouradian *et al.* 2008, Le Bas & Handley 1979, Zaitsev *et al.* 1998, Jones *et al.* 1996, Xie *et al.* 2009) that Ba and REE tend to be enriched toward the final stages of evolution in the carbonatite magma. Also, apatite is the most persistent mineral in the carbonatite evolution range, and P_2O_5 contents can be a useful tool to measure the differentiation degree, except perhaps in the final stages, where phosphorus may be associated with the late-stage crystallization of monazite.

Figure 3 shows P, Ba, and REE variation for different carbonatite compositional groups (see Table 1), indicating the progress of each group based on mineral paragenesis and overall chemical composition. The groups C1, C2, C3, and C5 evolved mostly by enrichment in BaO and depletion in P_2O_5, while the group C4 contains carbonatites with higher concentrations of REE.

Figure 4 shows a general evolution by increase in Ba, Sr, and REE, where C5 is located in an intermediate position, in the case of REE.

MAJOR ELEMENTS

The evolution sequences inferred from the mineral paragenesis and chemical changes observed in Figures 3 and 4 were used to establish a sequential arrangement of samples in each group (see suplementary data in Appendix 1) .The mineralogy present in these samples was then used to search for an index that could proxy for magmatic evolution of the studied carbonatites. Figures 5 to 11 show the behavior of several major element oxides with BaO/(BaO+SrO) as an evolution index.

The C1 and C2 carbonatites from Jacupiranga (Fig. 5) show an evolution similar to that of the corresponding, most primitive carbonatite group of the APIP (Fig. 6). C1a and C1b from Jacupiranga largely overlap in the region with low

values of BaO/(BaO+SrO), not exceeding 0.24, as expected for primitive compositions. The C1a cumulates show some positive correlation of BaO/(BaO+SrO) with REE and Na_2O resulting from apatite accumulation, whereas the mostly residual C1b carbonatites show the opposite behavior as a result of apatite removal. CaO and MgO present an erratic behavior.

The APIP C1 calciocarbonatites (Fig. 6) evolve with an increase in BaO and CO_2, indicating the increased amount of carbonate in the rock. The BaO content is very low relative to other APIP carbonatites, reaching a maximum at around 0.5%. K_2O, REE, and P_2O_5 decrease with C1 evolution. Both REE and P_2O_5 are controlled only by apatite fractionation at these early stages, while K_2O is controlled by phlogopite fractionation. CaO and MgO have mutually opposite behaviors, although with considerable scattering, and their distribution is probably controlled by independent factors, such as the removal of these elements from magma during fractionation of apatite and silicates, and its accompanying increase in carbonate enrichment. Furthermore, the opposite CaO and MgO trends may be associated with the presence of small, but varying amounts of dolomite in the rock. The sodium content is usually very low and independent of the stage of evolution of these rocks. One extreme Na_2O content of about 0.8% can be explained by the presence of amphibole.

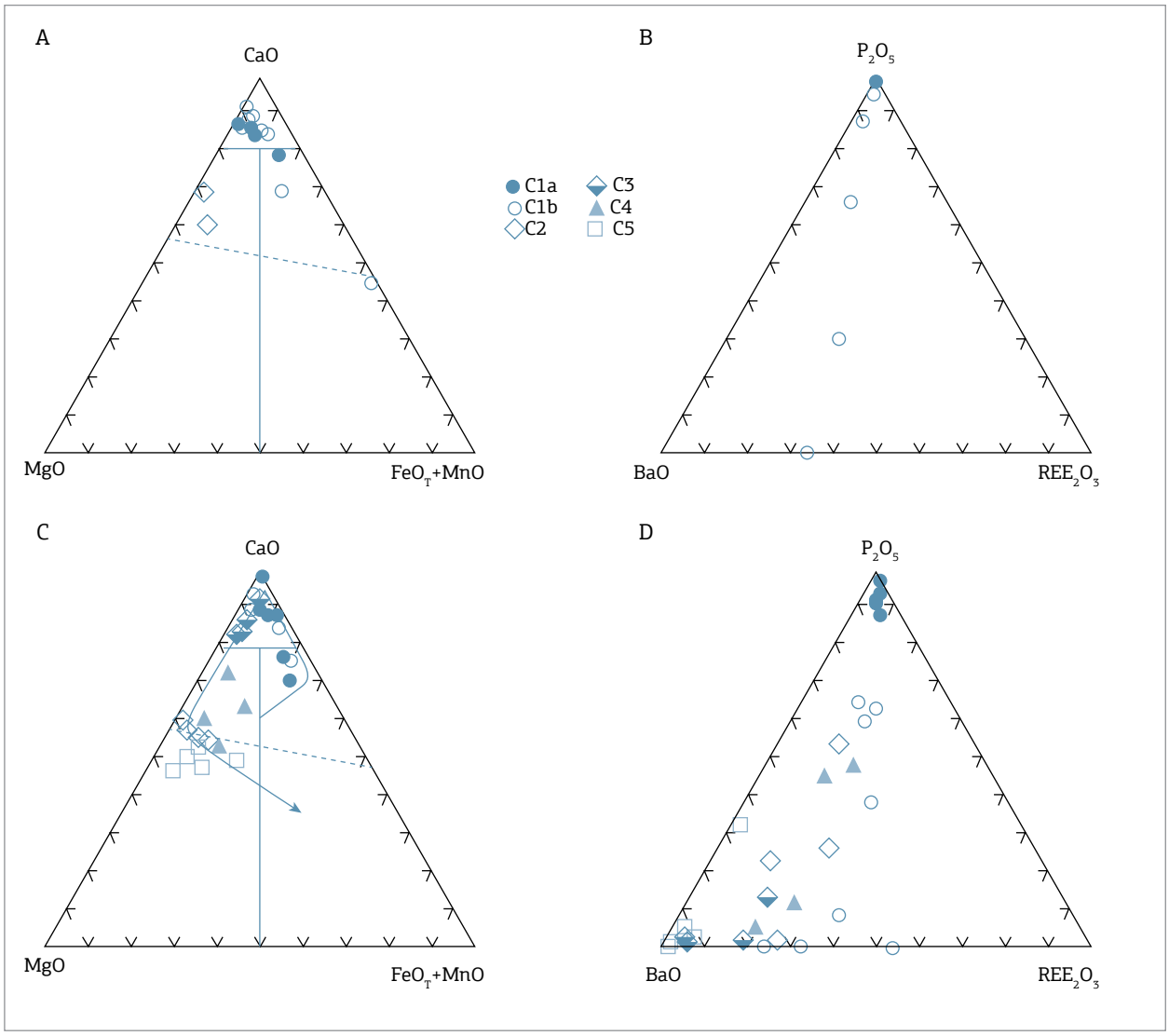

Figure 3. Carbonate classification diagram after Wooley and Kempe (1989) for the studied samples. The arrows indicate possible evolution trends for the Alto Paranaíba Igneous Province carbonatites (Ribeiro *et al.* 2014). Dashed line connects the compositions of pure dolomite and pure ankerite. (A) Jacupiranga, (C) Alto Paranaíba Igneous Province. P_2O_5 x BaO x REE_2O_3 diagram, in which C1, C2, C3, and C5 evolve from P_2O_5 toward BaO enrichment, but C4 evolves in the opposite direction (from BaO to P_2O_5). (B) Jacupiranga, (D) Alto Paranaíba Igneous Province.

The APIP C2 magnesiocarbonatites (Fig. 7) are characterized by the increase in BaO with evolution, although the levels of Ba are still relatively low when compared with other magnesiocarbonatites. The CaO content is insensitive to evolution, reflecting the scarcity or absence of calcite in these rocks. The P_2O_5 content is low (maximum 0.2%), but systematically decreases, signaling apatite fractionation. The similar behavior of SrO and Na_2O is probably also related to the apatite removal. It is important to note that, unlike C1, the calcite is absent or very rare in C2 carbonatites, which implies a control of the SrO content by fractionating apatite, since strontium does not enter the structure of dolomite easily.

In our studied sample set, the C3-type carbonatites are restricted to samples from the Tapira Complex. In this group, there is no obvious control of fractionating apatite on the content of P_2O_5, which shows erratic variation (Fig. 8). BaO, MgO, Na_2O, and, less obviously, REE increase with magmatic evolution whereas CaO and SrO decrease, suggesting that calcite crystallization gives way to other carbonates such as norsethite ($BaMg(CO_3)_2$) and, more rarely, baritocalcite ($BaCa(CO_3)_2$) with magma evolution. The atypical behavior of CO_2, which increases slightly at first and then constantly decreases, is possibly related to the same mineralogical effect, because carbonates containing heavy elements such as Ba, Sr, and REE will naturally have a lower CO_2 proportion by weight. The BaO (up to 13%) and SrO (up to 5%) levels are substantially greater than that in C1 and C2 carbonatites. The contents of K_2O are low and decrease very quickly in the early evolution of

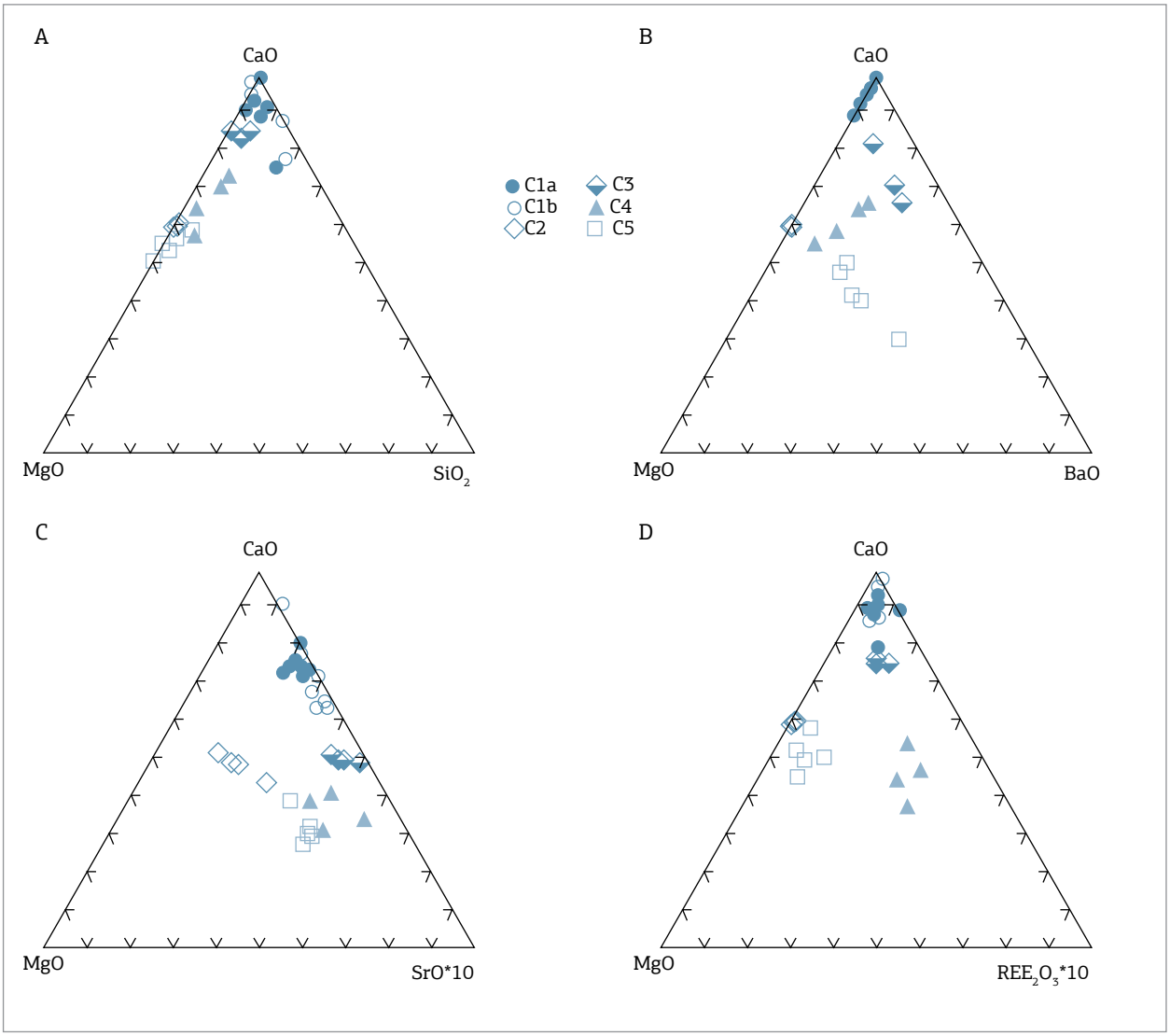

Figure 4. Graphical representation of CaO x MgO x (A) SiO_2, (B) BaO, (C) SrO, and (D) REE_2O_3. C1, C2, C3, C4, and C5 evolve from CaO toward MgO and BaO; C1 and C3 evolve from CaO toward SrO; and C2, C4, and C5 evolve from MgO toward SrO. C4 and C5 present the most REE_2O_3 content.

C3, indicating total consumption of phlogopite as the silicate formed at this stage.

The C4 magnesiocarbonatites occur in Salitre, Araxá, and Tapira, and are characterized by the presence of monazite, instead of carbonates, as the main REE mineral. This fact is illustrated by the high REE content (up to 2.5%, Fig. 9) in carbonatites of this group and confirmed by SEM and electron microprobe (EPMA) analyses. In addition to REE, there is an increase in K_2O, Na_2O, and MgO, followed by an important decrease in the concentration of BaO, CaO, and CO_2 with magma evolution. A notable characteristic is the negative correlation between BaO and REE, which is not observed in the other groups.

The C5 magnesiocarbonatites are from Catalão I, Catalão II, Araxá, and Tapira, and show increase in BaO, SrO, Na_2O, and CO_2, and decrease in CaO and K_2O with evolution (Fig. 10). Some of the less evolved samples of this group have very high P_2O_5 (up to 8–9%) and phosphorus contents are strongly controlled by the apatite fractionation at the early stages. This fact contrasts with the low phosphorus observed in C2, and suggests that carbonatites from C5 represent a distinct magmatic pulse. The strong increase in BaO, SrO, and Na_2O indicates the crystallization of rare or complex carbonates such as norsethite, burbankite, and strontianite, whose occurrence is confirmed in electron microscopy and electron microprobe analyses. The replacement of dolomite by these other carbonate minerals as the main crystallizing phases in the magma explains most of the observed chemical changes, including a consistent decrease in CaO, but does not explain the progressive increase in CO_2. At the current stage, the reasons for this behavior are not clear.

Applying the same classification concepts to APIP carbonatite analyses from literature (Grasso 2010, Brod 1999, Traversa *et al.* 2001, Palmieri 2011, Barbosa 2009, Cordeiro 2009, Gomes & Comin Chiaramonti 2005,

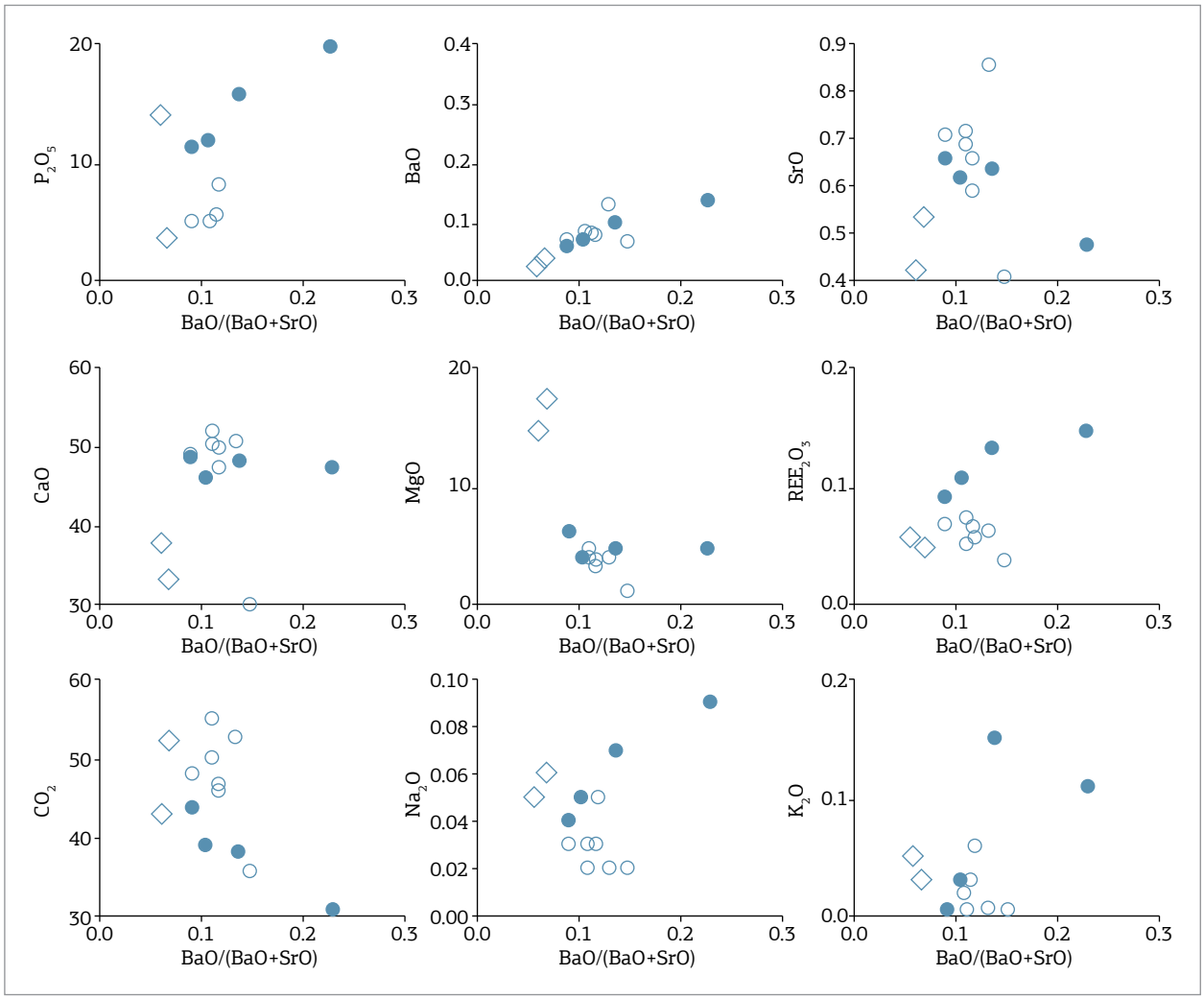

Figure 5. Behavior of selected major element oxides with magma evolution for the Jacupiranga C1 calciocarbonatites and C2 magnesiocarbonatites. Symbols used are same as in Figure 3.

Araújo 1996, Morbidelli *et al.* 1997, Machado Junior 1992), it was possible to build compositional fields for the province. The general trends for the province (Figs. 11 and 12) are similar to those described previously for our samples, such as increase in BaO and CO_2, and decrease in K_2O and P_2O_5 with evolution. Possible exceptions are some C1a apatite-rich cumulate rocks with anomalously high P_2O_5, associated with the fractionation of apatite, but not clear for the province as a whole.

The C2 samples from this work are plotted inside the APIP carbonatite fields (Fig. 12), except for the CO_2 and SrO contents of some samples that cover slightly larger areas. In general, the classification fits well, maintaining the trends described for this group, such as increase in BaO and REE contents, whereas CaO is insensitive to evolution, and P_2O_5 content is low.

Samples from the C3 group (Fig. 11) fit very well to the province fields. BaO, MgO, and Na_2O increase whereas CaO, SrO, K_2O, and CO_2 decrease in the entire province, following the behavior described for this group from our samples. The P_2O_5 content is low and insensitive to magma evolution.

The C4 group samples (Fig. 12) plot mostly inside the province fields or following the same trend. Available data for carbonatites with C4 characteristics in the whole province are scarce generating a restricted field, but even in this case the samples from our data set and from the whole province have very similar chemical behavior which strengthens the efficiency of the devised classification scheme. The whole province C4 trends are marked by high REE content, an increase in K_2O and Na_2O, and a decrease in the concentration of BaO, CaO, and CO_2.

The C5 group shows only partial coincidence between the compositional range of our data set and the whole province, suggesting that our samples have a more extreme composition, particularly for BaO. However, even when

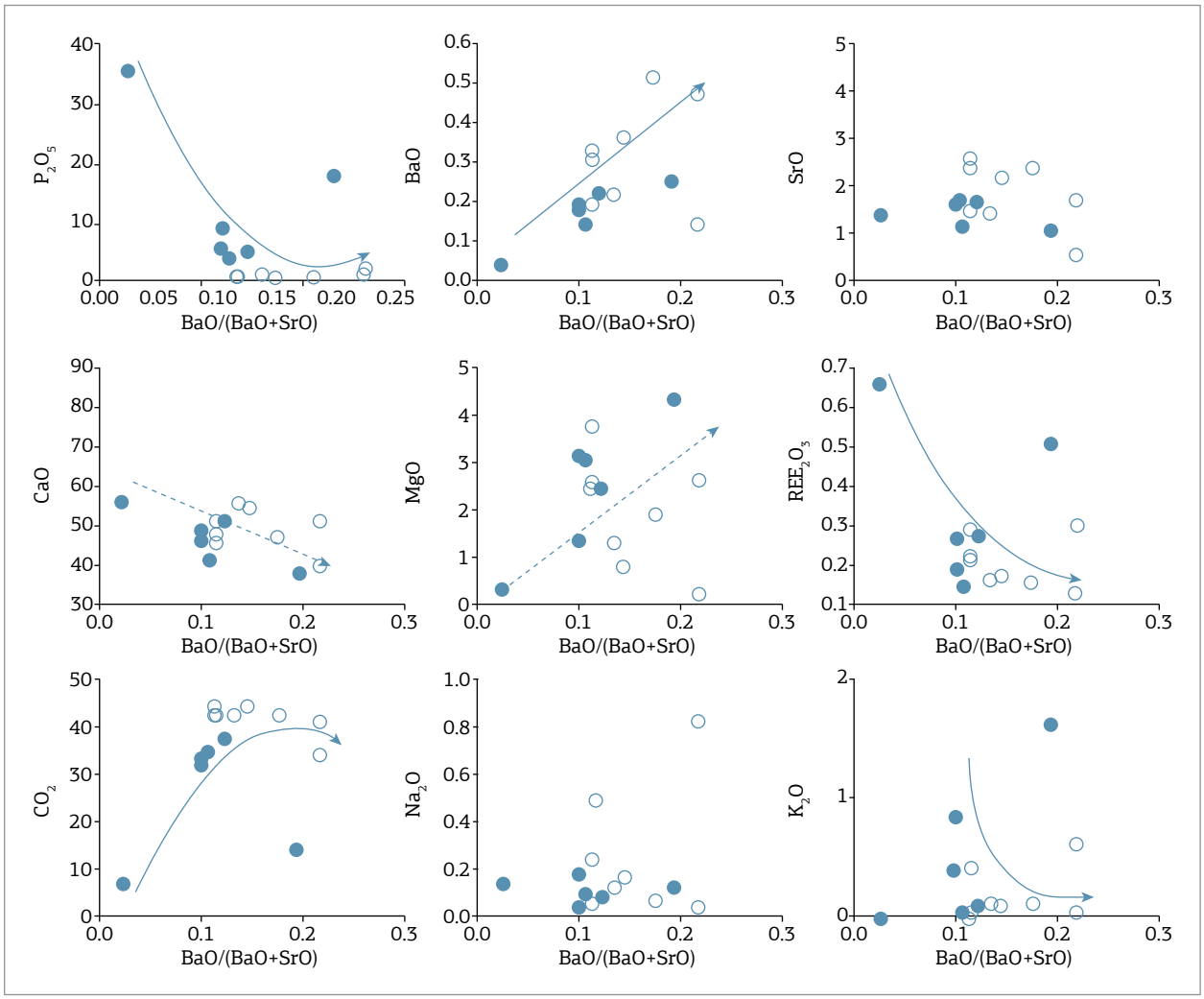

Figure 6. Behavior of selected major element oxides with magma evolution for the Alto Paranaíba Igneous Province C1 calciocarbonatites. Symbols used are same as in Figure 3.

the fields do not coincide, the two trends are similar. This group shows an increase in BaO, Na_2O, and CO_2 contents, and a decrease in SrO, CaO, REE, CO_2, and K_2O with magmatic evolution.

TRACE ELEMENTS

Trace elements in the carbonatite magma may be greatly affected by specific late-stage fractionating phases such as sphene, apatite, perovskite, monazite, or zircon (e.g. Nelson *et al.* 1988). Pyrochlore and baddeleyite, which are additional common phases in our sample set, may also have a great effect on some trace elements such as the high field strength elements (HFSE and REE). Liquid immiscibility is another important process affecting trace element distribution in carbonatites and associated rocks, including changes in geochemically similar element pairs such as Nb–Ta, Zr–Hf, and REE (e.g. Hamilton *et al.* 1989, Veksler *et al.* 1998, 2012, Brod *et al.* 2013).

$La_{(n)}/Yb_{(n)}$ tends to increase with magma evolution (Fig. 13) within the same carbonatite group and, in most cases, between different groups. Group C5 is an exception, since most samples have lower $La_{(n)}/Yb_{(n)}$ for high BaO/(BaO+SrO), $U_{(n)}/Th_{(n)}$ decreases with evolution in C1 group with significant fractionation, which may reflect the crystallization of pyrochlore.

The $Nb_{(n)}/Ta_{(n)}$ ratio show complex behavior, and its variation shown in Figure 13 does not seem to be affected by fractional crystallization, since the variability of the Nb/Ta ratio is far greater than that of the BaO/(BaO+SrO). Brod *et al.* (2013) have shown that liquid immiscibility in the Tapira complex of the APIP

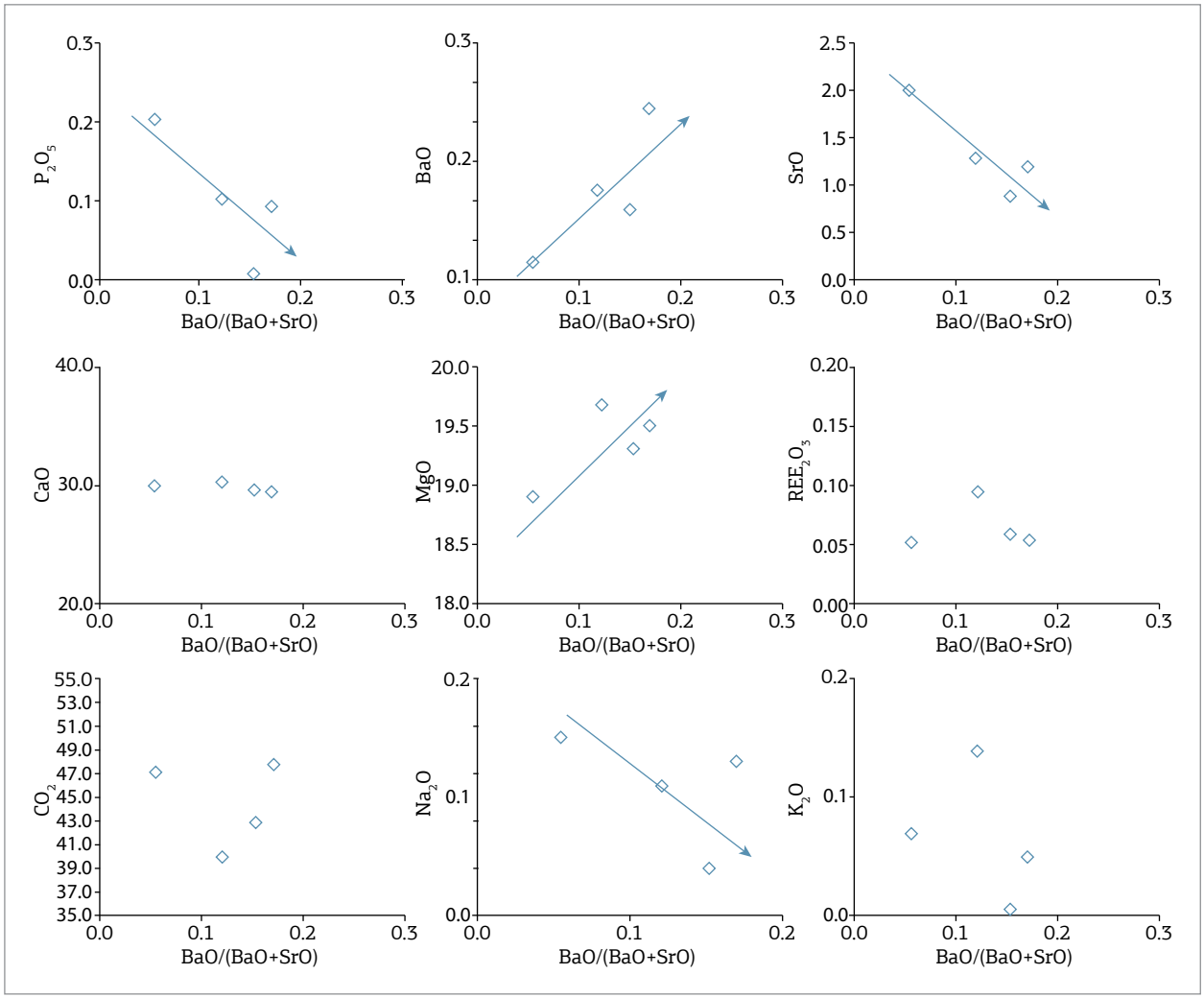

Figure 7. Behavior of selected major element oxides with magma evolution of the Alto Paranaíba Igneous Province C2 magnesiocarbonatites. Symbols used are same as in Figure 3.

resulted in the increase of the $Nb_{(n)}/Ta_{(n)}$ ratio of the carbonate conjugate, sometimes by several orders of magnitude, if compared with the same ratio in the parental liquid. In our data set, most samples from C1a and some samples from C5 show values near 1.3, which is the $Nb_{(n)}/Ta_{(n)}$ ratio of the parental magma of the APIP complexes (Brod *et al.* 2013). For the other samples, the high values of $Nb_{(n)}/Ta_{(n)}$ ratio suggest that they have been involved in liquid immiscibility at some point in their evolution, according to Brod *et al.*'s (2013) detection and definition. The fact that there are variable $Nb_{(n)}/Ta_{(n)}$ within a single group suggests that both crystal fractionation and liquid immiscibility played a role in magma evolution in most cases. $Sc_{(n)}/Y_{(n)}$ displays an interesting behavior, allowing an efficient separation of groups C2 and C5, which show high values of this ratio.

MULTIELEMENT DIAGRAMS AND RARE EARTH ELEMENTS

Figure 14 shows chondrite-normalized multielement diagrams (Thompson 1982). The C1 carbonatites, both from Jacupiranga and the APIP, may be divided into

- carbonatites containing cumulus apatite, characterized by a positive anomaly in phosphorus and
- residual carbonatite from fractional crystallization processes, which have a negative P anomaly.

According to this criterion alone, most C1b carbonatites from Jacupiranga should be considered apatite-rich cumulates. However, the behavior of other major and trace elements, as well as the distinct REE patterns between Jacupiranga C1a and C1b, supports the proposed division.

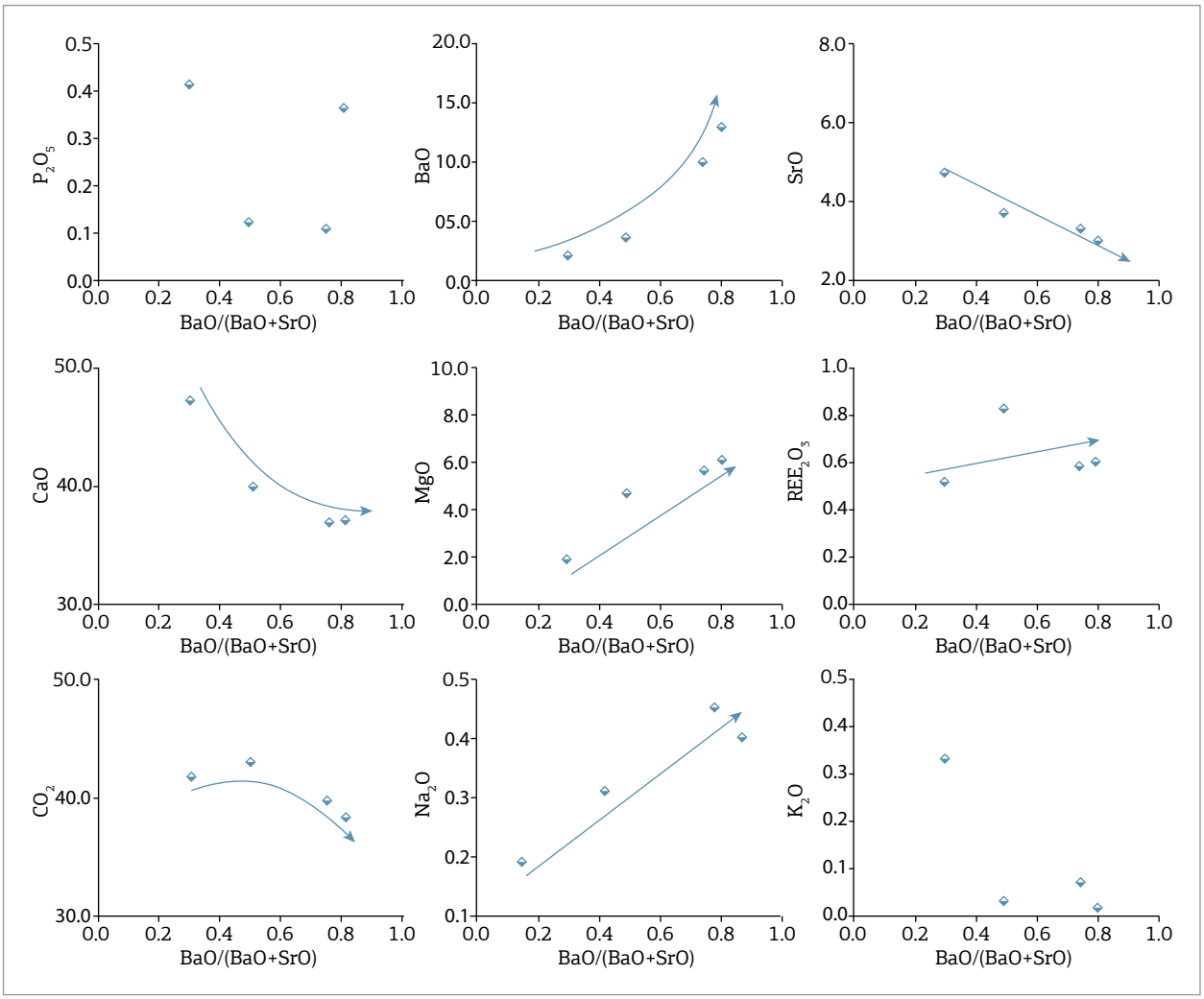

Figure 8. Behavior of selected major element oxides with magma evolution for the Alto Paranaíba Igneous Province C3 calciocarbonatites. Symbols used are same as in Figure 3.

In Jacupiranga, the chondrite-normalized Nb/Ta are typically lower than 1 in C1 and higher than 1 in C2, although the differences are relatively small. In the APIP data set, C1b shows values of chondrite-normalized Nb/Ta significantly higher than most C1a samples, suggesting that liquid immiscibility may have played a role at a differentiation stage as early as C1b very early differentiation stages.

The two C1 subgroups may be recognized in chondrite-normalized rare earth elements diagrams (Fig. 14). The apatite-rich cumulates show higher REE concentrations, especially from medium and light REE, indicating that apatite is a major REE carrier at this stage in both Jacupiranga and the APIP. The $La_{(n)}/Lu_{(n)}$ ratio of C1a from Jacupiranga is in the range of 52 – 92, whereas in C1b this ratio is in the range of 22 – 46. In the APIP early-stage carbonatites, $La_{(n)}/Lu_{(n)}$ ranged from 100 to 250 in C1a and from 35 to 140 in C1b.

In the C2 magnesiocarbonatites, the Jacupiranga samples show a positive P anomaly, indicating apatite accumulation, whereas the APIP samples always show a negative P anomaly, indicating that they are residual carbonatites. Regarding the chondrite-normalized Nb/Ta ratio, the Jacupiranga C2 shows values close to or lower than 1, suggesting that liquid immiscibility was not involved in their generation. Only two APIP samples have available Ta data. Both presents relatively high Nb/Ta, reaching up to 19, indicating that they are the product of immiscible liquids.

$La_{(n)}/Lu_{(n)}$ ratio of the C2 magnesiocarbonatites ranges from 136 to 362 in the APIP and from 41 to 50 in Jacupiranga. Both C1 and C2 group in the carbonatites of the APIP have total contents of REE higher than their equivalents in Jacupiranga, suggesting that the REE enrichment is a Province-related characteristic.

The C3 calciocarbonatites show a negative P anomaly and high chondrite-normalized Nb/Ta ratio (31–53), which indicates a relatively evolved carbonatite generated by liquid

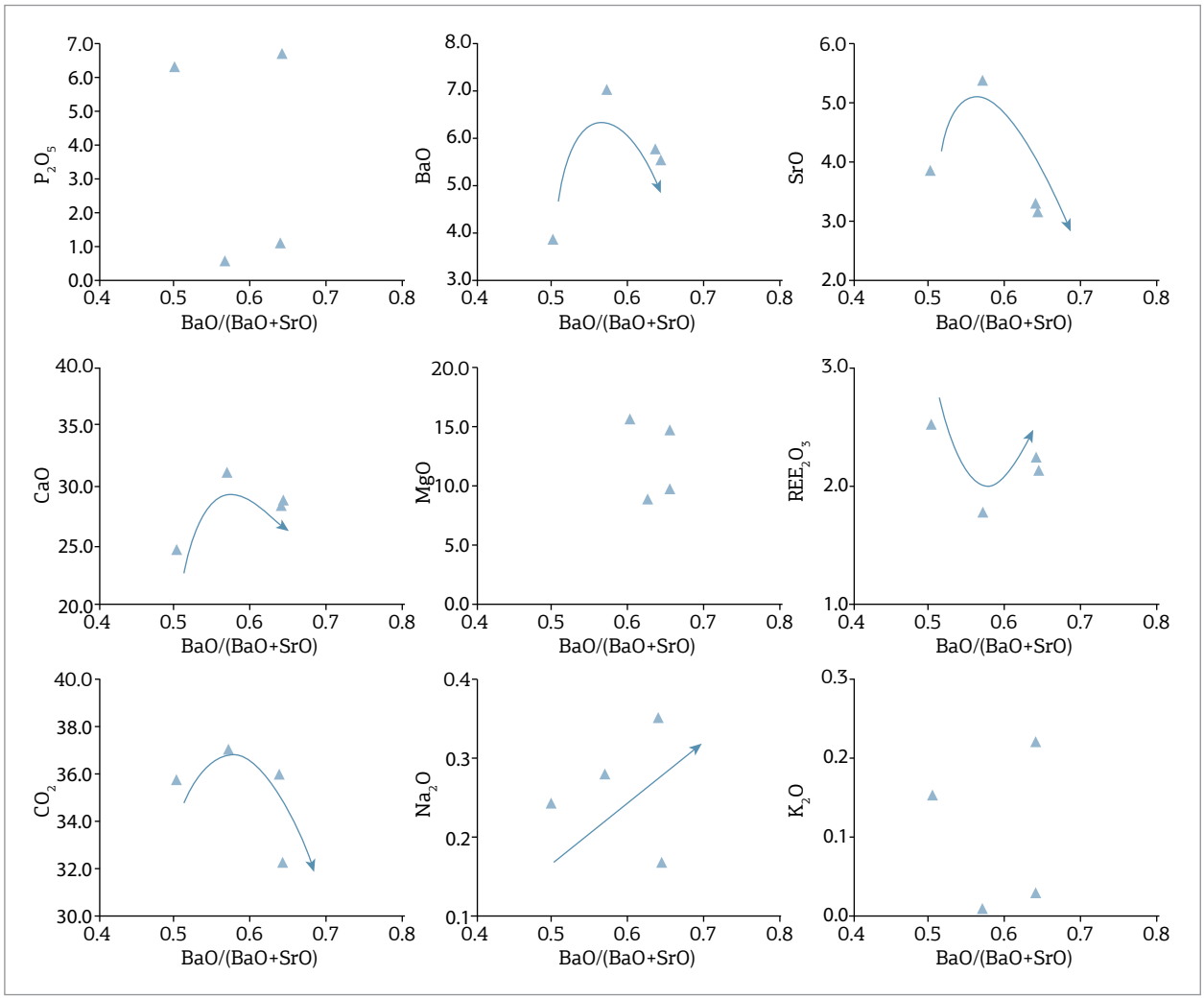

Figure 9. Behavior of selected major element oxides with magma evolution from the Alto Paranaíba Igneous Province C4 magnesiocarbonatites. Symbols used are same as in Figure 3.

immiscibility and that underwent apatite fractionation. Their $La_{(n)}/Lu_{(n)}$ ratio ranges between 178 and 354, similar to C2 and slightly higher than C1.

The C4 magnesiocarbonatites exhibit a $Nb_{(n)}/Ta_{(n)}$ ratio ranging from 5 to 40 and a negative P anomaly indicating the involvement of liquid immiscibility and the fractionation of apatite at an earlier stage of magmatic evolution. The samples of this group also have a slight negative Sr anomaly, which may be explained by fractionation of Sr-rich carbonates, such as strontianite or even Sr-rich calcite at an earlier stage. Alternatively, this characteristic may be an artifact of the monazite enrichment observed in C4. The REE diagram (Fig. 14) shows a strong LREE/HREE fractionation ($La_{(n)}/Lu_{(n)}$ values between 520 and 1515).

The magmatic evolution of the C5 group also involved immiscibility, in most cases, with the $Nb_{(n)}/Ta_{(n)}$ ratio reaching a maximum of 37. Part of the C5 sample set shows negative P anomaly, indicating prior apatite fractionation. The REE diagram (Fig. 14) shows a very strong LREE/HREE enrichment, the $La_{(n)}/Lu_{(n)}$ ratio ranging from 180 to 1635.

STABLE ISOTOPES (C, O, S)

Figure 15 depicts the C, O, and S stable isotope composition. The C and O data were obtained from carbonates, using a Delta V Plus gas source mass spectrometer at the Geochronoly Lab, University of Brasília, after 1 hour reaction, using Gas Bench at 72°C, with phosphoric acid. No correction was used because at this temperature there is no need to do it (Spotl & Vennemann 2003). The C isotopic data were obtained by Gomide *et al.* (2013) in sulfides. The values are expressed in δ notation per thousand (see calculation in chapter 1) compared to the Vienna Pee Dee Belemnite (V-PDB) reference standards for C, Standard Mean Ocean Water (SMOW) for O, and Vienna Canyon Diablo Troilite (V-CDT) for S.

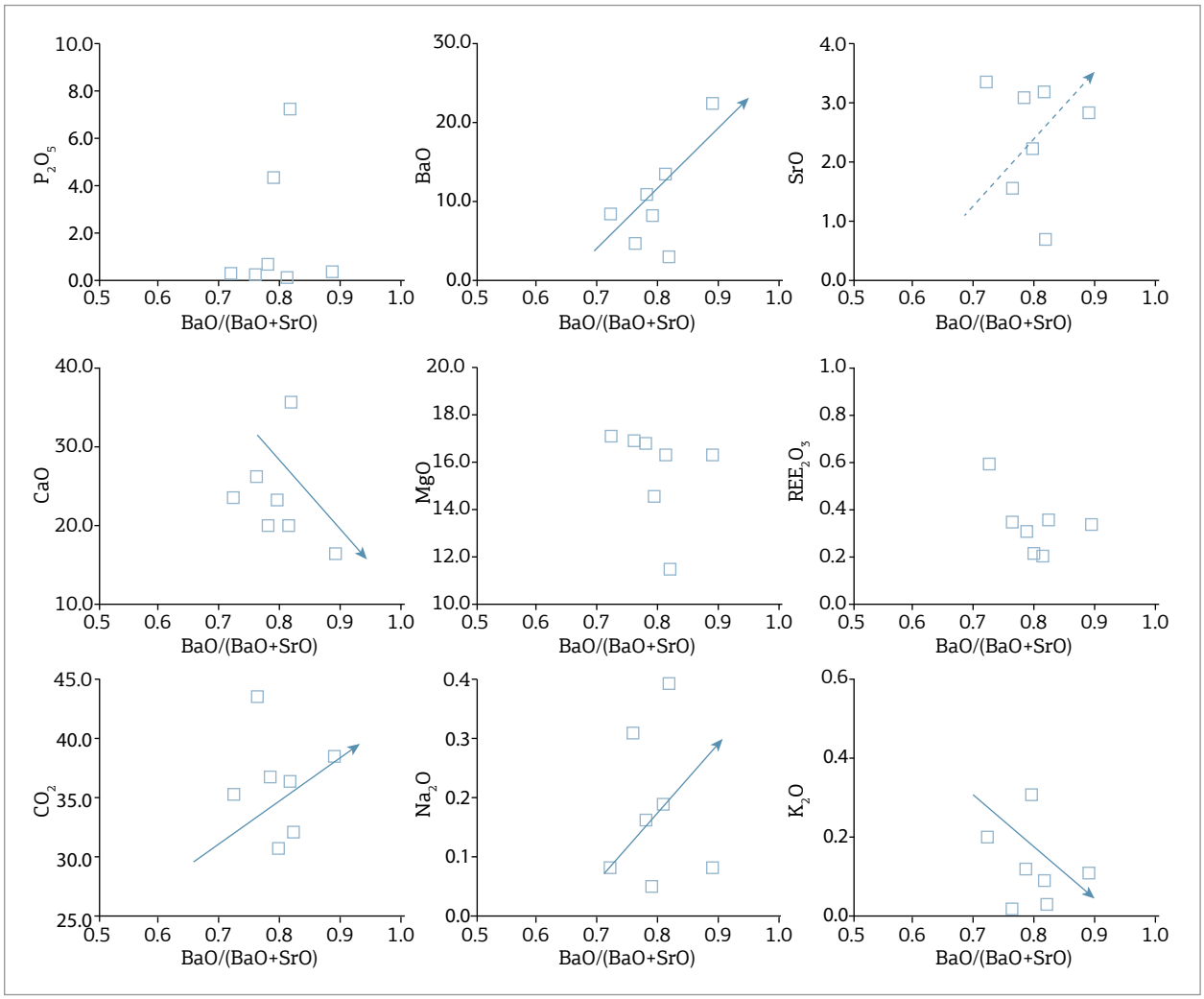

Figure 10. Behavior of selected major element oxides with magma evolution in the Alto Paranaíba Igneous Province C5 magnesiocarbonatites. Symbols used are same as in Figure 3.

The Jacupiranga samples show a C and O isotopic composition that evolves according to Rayleigh fractionation. All Jacupiranga samples plot inside the range are defined as mantle values (Taylor *et al.* 1967).

Similarly to Jacupiranga, the C1 from the APIP show a C and O isotopic evolution by magmatic fractionation and all the samples have values consistent with the mantle range. The C2 also show isotopic evolution consistent with magma fractionation, but reach higher $\delta^{18}O$ values, slightly exceeding the mantle range. Some C2 samples suggest hydrothermal alteration trends, with a shift to high $\delta^{18}O$ values at relatively constant $\delta^{13}C$.

C3 follow a magmatic fractionation trend, but one sample has a shift to higher $\delta^{18}O$ values suggesting that it has been affected by hydrothermal alteration.

The C4 exhibit two trends, both starting within the mantle composition range. One trend evolves into heavier C and O isotopic compositions, typical of magmatic fractionation or of interaction with fluids rich in both H_2O and CO_2, whereas the other evolves by increasing $\delta^{18}O$ at relatively constant $\delta^{13}C$, indicative of hydrothermal alteration.

The C5 also show two evolution trends, analogous to those observed in C4 and interpreted in the same way as

1. indicative of magmatic fractionation or interaction with carbohydrothermal fluids interaction and
2. hydrothermal alteration.

Santos and Clayton (1995) interpreted C and O isotopic differences between carbonatites from Jacupiranga and from the APIP as a result of different levels of intrusion.

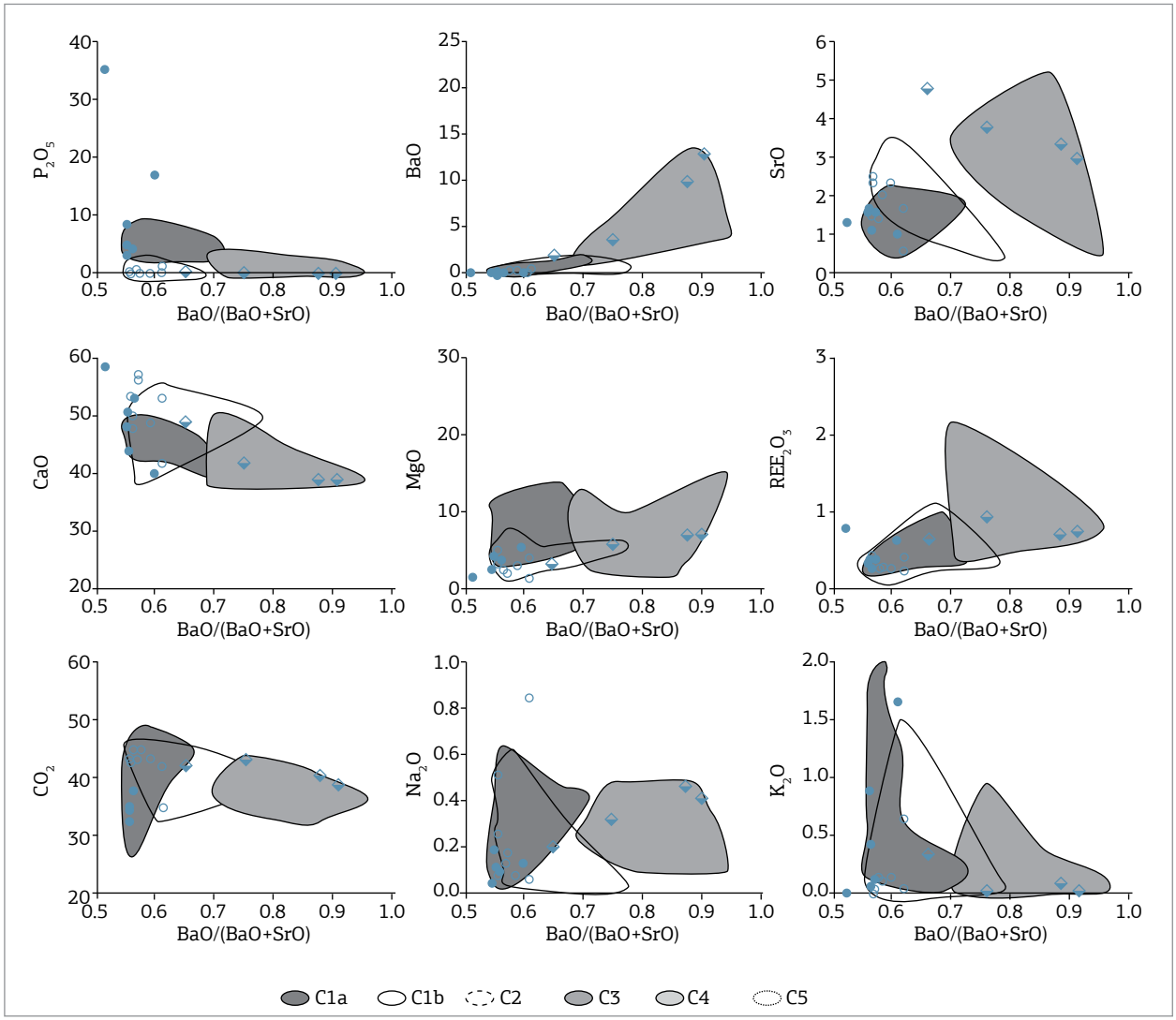

Figure 11. Behavior of selected major element oxides with magma evolution for the Alto Paranaíba Igneous Province C1 and C3 calciocarbonatites, samples from this work compared with all province data (Grasso 2010, Brod 1999, Traversa *et al.* 2001, Palmieri 2011, Barbosa 2009, Cordeiro 2009, Gomes & Comin-Chiaramonti 2005, Araújo 1996, Morbidelli *et al.* 1997, Machado Junior 1992). Symbols used are same as in Figure 3.

In that model, Jacupiranga carbonatites crystallized in a deeper-seated magma chamber are less evolved and have more restricted isotopic compositions. The APIP carbonatites would have been emplaced in much shallower chambers, the lower lithostatic pressure allowing for a greater variety of differentiation processes. Our data are consistent with the interpretations of Santos and Clayton (1995). We interpret the APIP C1, C2, and C3 carbonatites as representing less evolved magmas, while C4 and C5 formed at later stages and therefore were more susceptible to processes such as degassing and subsequent hydrothermal and carbohydrotermal alteration. However, some interaction with external fluids cannot be ruled out, especially in the cases of $\delta^{18}O$-only variation.

Regarding the coupled variation in S and O isotopes, the Jacupiranga samples plot in a very restrict interval, compatible with mantle composition. The small composition ranges do not allow the definition of conclusive trends.

In the APIP samples, all groups show S isotopic composition compatible with the mantle range, except for a few C5 samples showing textural evidence of sulfur degassing and/or hydrothermal alteration (Gomide *et al.* 2013).

The APIP C1 show higher $\delta^{34}S$ values, on average, than the C2, and the latter define a clearly decreasing trend of $\delta^{34}S$, which is consistent with the observation that the $\delta^{34}S$ values in sulfides decrease with magmatic evolution of each complex (Gomide *et al.* 2013). Although the carbon-oxygen diagram suggests that some samples from this group were

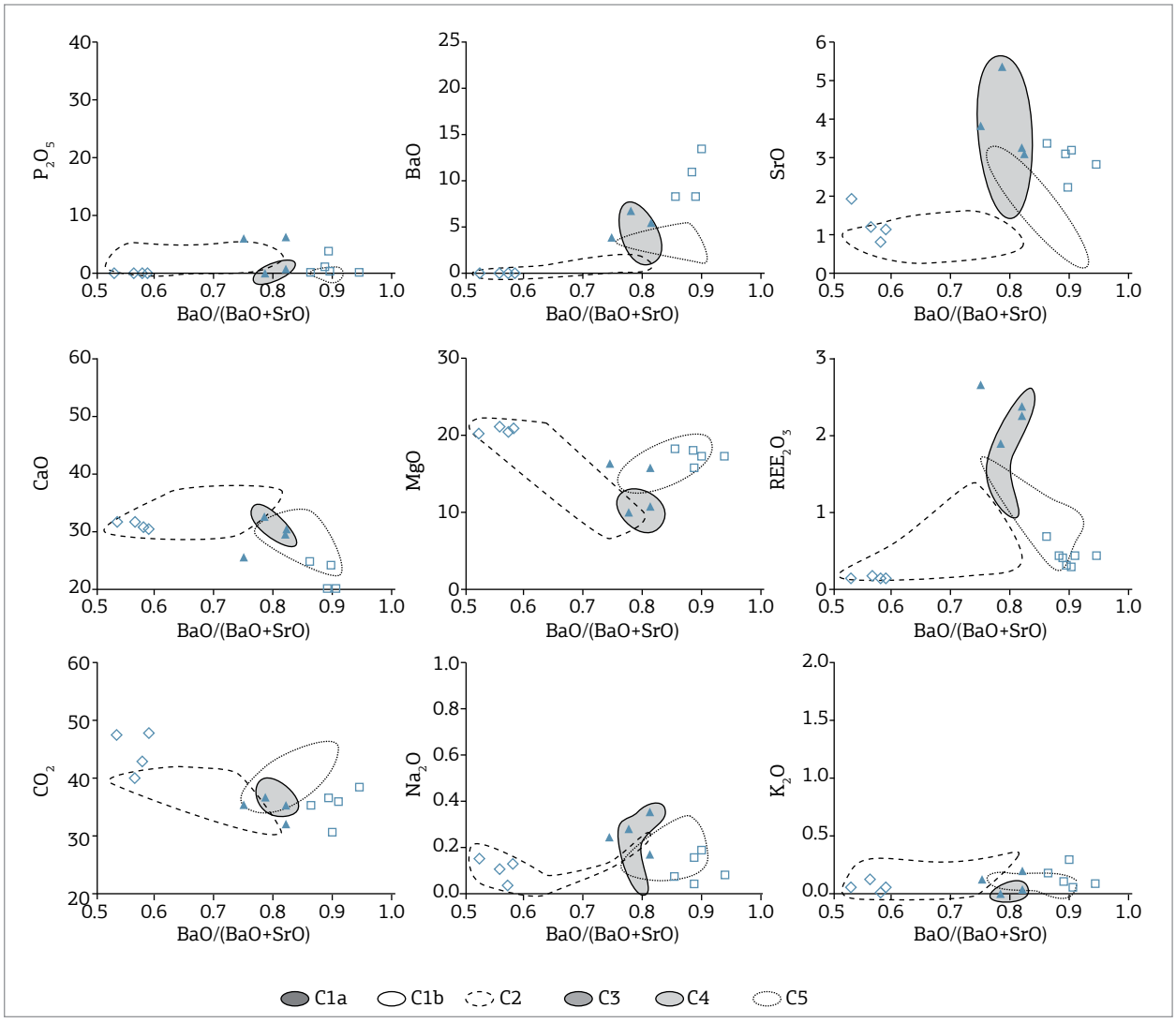

Figure 12. Behavior of selected major element oxides with magma evolution for the Alto Paranaíba Igneous Province C2, C4, and C5 magnesiocarbonatites, samples from this work compared with data from the whole province (Grasso 2010, Brod 1999, Traversa *et al.* 2001, Palmieri 2011, Barbosa 2009, Cordeiro 2009, Gomes & Comin-Chiaramonti 2005, Araújo 1996, Morbidelli *et al.* 1997, Machado Junior 1992). Symbols used are same as in Figure 3.

possibly affected by hydrothermal alteration, the sulfur isotopes appear to be unaffected by this process.

The C4 samples with petrographic evidence of sulfur degassing (Gomide *et al*. 2013) are aligned along two positive correlation lines in the $\delta^{34}S$–$\delta^{18}O$ diagram. Similar correlations are observed in the other groups (C1a, C3, and C4), and it is possible that this feature is a sulfur degassing characteristic. However, the joint behavior of S and O isotopes still needs to be studied in more detail, because the relationship between these two systems probably is not trivial. For example, the two elements participate in multiple minerals (carbonates, oxides, silicates, sulfates, and sulfides) may be degassed as distinct species (CO_2, H_2S, SO_2) at different times during magmatic evolution and are sensitive to variations in the oxidation state of the system.

CONCLUSIONS

A major difficulty in the study of carbonatite magmatism is to establish a numerical parameter for gauging magmatic evolution, analogous to differentiation indexes used in the study of silicate magmas, against which to measure other geochemical, isotopic, mineralogical, and textural properties. This work proposes an integrated method of assessment of the magmatic differentiation stage in carbonatites of the APIP. The studied carbonatites were classified into the successively more evolved groups C1 to C5. The evolution of groups C1, C2, C3, and C5 may be monitored by BaO enrichment and P_2O_5 depletion, whereas C4, a group of REE-rich carbonatites, evolves through enrichment of both rare earths and phosphorus.

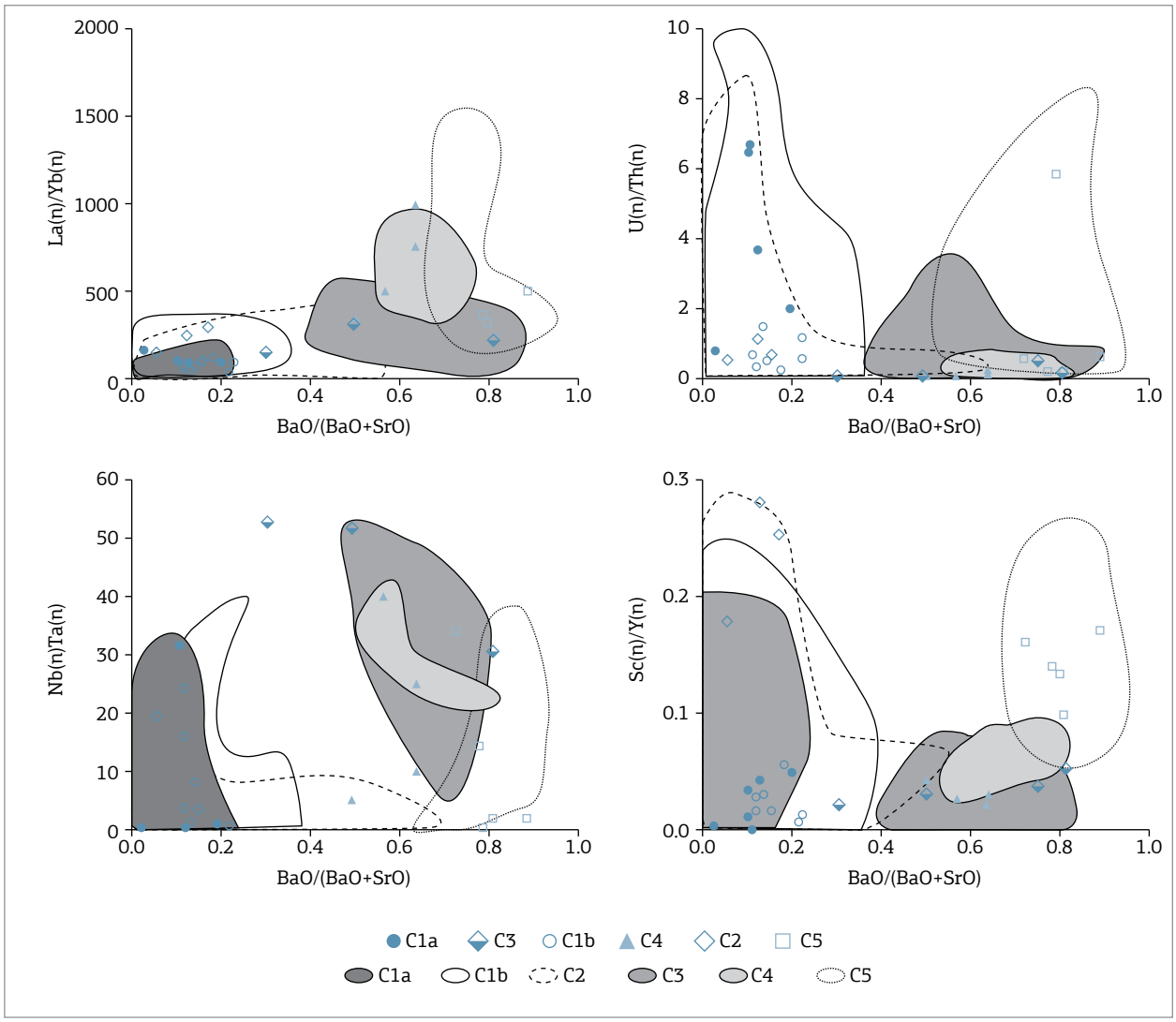

Figure 13. Trace elements behavior of some key chondrite-normalized elemental ratios for this work Alto Paranaíba Igneous Province samples compared with all province data.

In this work, we devise a differentiation index involving BaO and SrO, applied it to our sample set and to data for the APIP carbonatites from the literature.

The evolution of C1 calciocarbonatites results in increased calcite component in the magma, by the removal of apatite (including olivine, phlogopite, and magnetite). In our samples, this mostly produces apatite cumulates (C1a) and a residual carbonatite (C1b).

The C2 group consists of unevolved magnesiocarbonatites crystallizing apatite and dolomite, and may also represent cumulates (e.g. C2 samples from Jacupiranga) or residual carbonatite (e.g. C2 samples from the APIP).

The C3 in our sample set are all from the Tapira Complex. This group is characterized by fractionation of apatite, calcite, and phlogopite, leading to a residual concentration of Ba, Mg, and Na, and the crystallization of carbonates

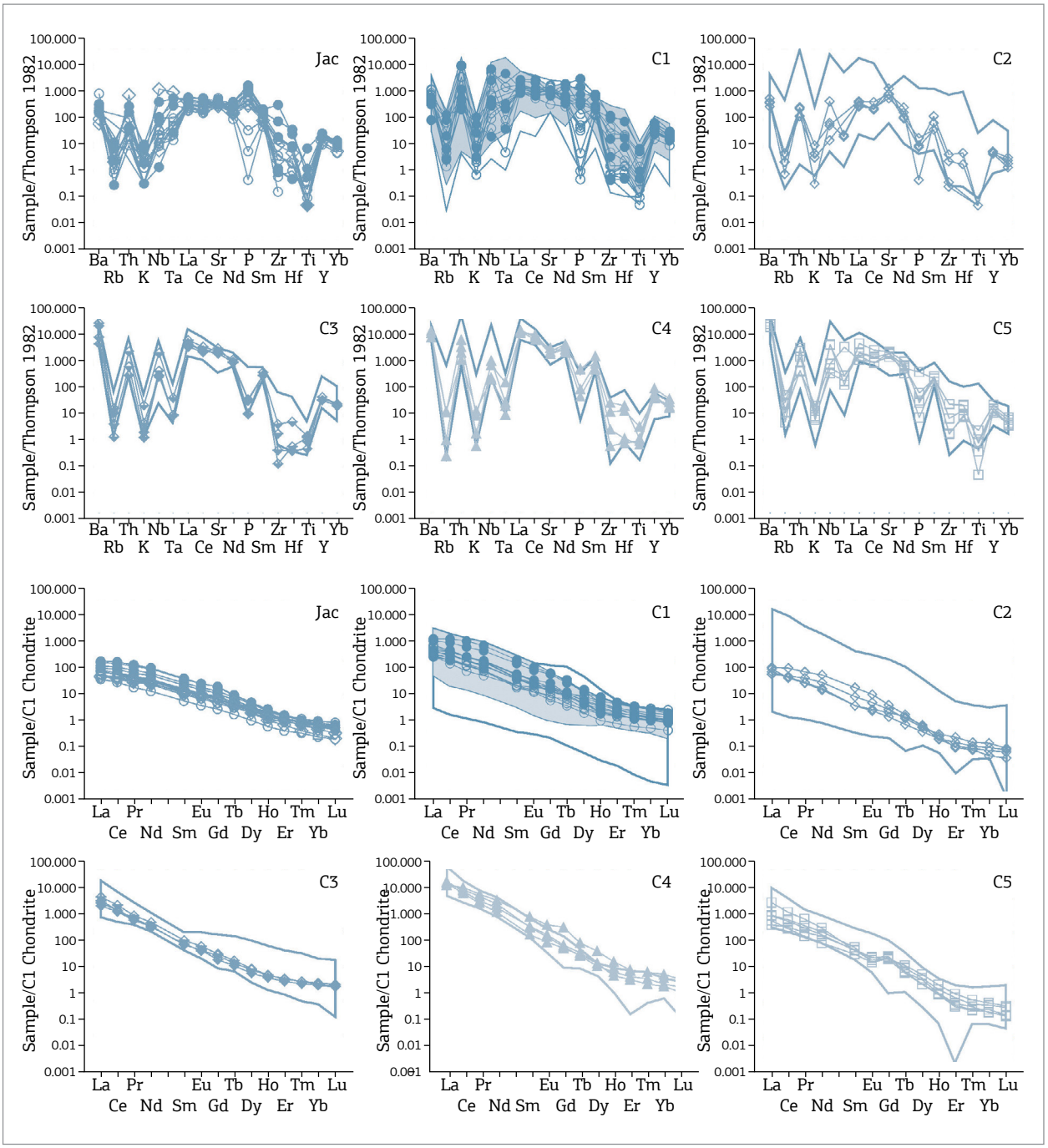

Figure 14. Multielement diagram for C1a, C1b, C2, C3, C4, and C5 carbonatites. The fields represent the province fields for each group and REE diagrams. The fields represent the Alto Paranaíba Igneous Province range for each group (gray = C1a, black outline = C1b). Symbols used are same as in Figure 3.

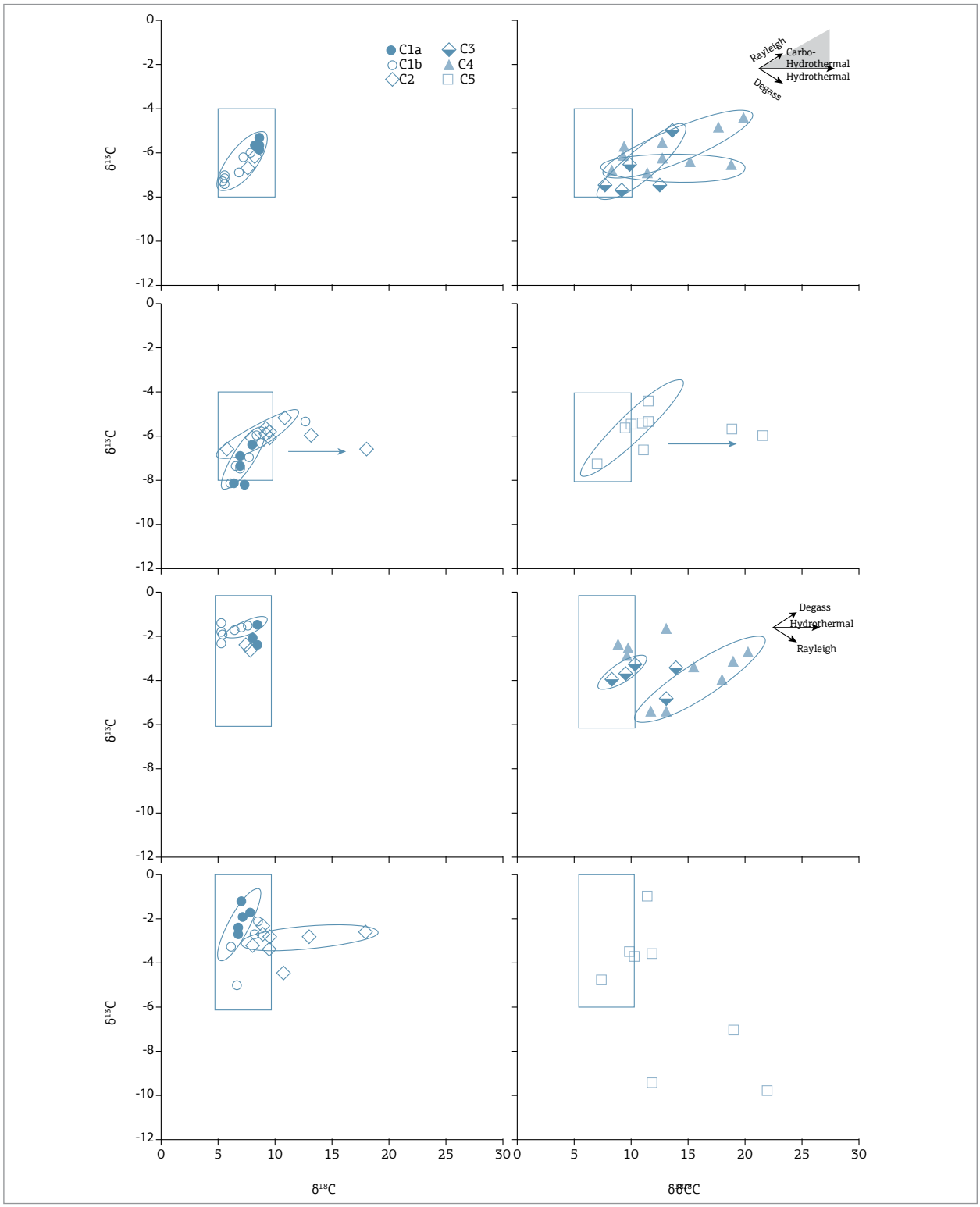

Figure 15. Left side: Stable isotope composition of carbon and oxygen in carbonates for Jacupiranga and for the Alto Paranaíba Igneous Province groups C1 to C5. Right side: Stable isotope compositions of sulfur in sulfides and oxygen in carbonates for Jacupiranga and for the Alto Paranaíba Igneous Province groups C1 to C5. The rectangular field corresponds to the isotopic composition of the mantle defined for C and O by Taylor *et al.* (1967) and for S by Deines (1989), Mitchell & Krouse (1975), Druppel *et al.* (2006) and Nikiforov *et al.* (2006). Arrows indicate changes expected in Rayleigh fractionation, low-temperature hydrothermal alteration without the participation of CO_2 and degassing (Taylor *et al.* 1967, Ray & Ramesh 2000). The gray triangle in the inset illustrates the expected variations (e.g. Santos & Clayton 1995) in low-temperature carbohydrotermal alteration with high H_2O:CO_2 (1,000:1) and variable fluid/rock ratios. The S isotope data are from Gomide et al. (2013), whereas C and O data are from this work.

such as norsethite, baritocalcite, and burbankite directly from the magma. This group marks the exhaustion of the silicatic component in calciocarbonatites, with the end of phogopitecrystallization. The C3 geochemical characteristics, in particular its high chondrite-normalized Nb/Ta and the strong negative Zr and Hf anomalies, indicate that these melts were produced by liquid immiscibility (e.g. Brod *et al.* 2013).

C4 consists of Ba-, Sr-, and REE-rich magnesiocarbonatites. The main liquidus phases are dolomite, Fe-dolomite, norsethite, and strontianite. Its distinctive characteristic is the strong enrichment in monazite, marked by a concomitant increase in P_2O_5 and REE_2O_3 with magmatic evolution. The geochemical characteristics indicate the involvement of liquid immiscibility in the evolution of these magmas.

The geochemical characteristics of the C5 indicate strong apatite and phlogopite fractionation, with decrease in CaO, P_2O_5, and K_2O, and enrichment in Ba, Sr, Na, and CO_2, resulting in a direct crystallization of strontianite and norsethite as liquid phases. Exsolutions indicates that the C5 carbonatites were crystallized in still relatively high-temperature conditions. The high chondrite-normalized Nb/Ta indicates the involvement of liquid immiscibility processes in the evolution of these magmas. Previous work (Junqueira-Brod *et al.* in prep., Gomide *et al.* 2013) identified degassing of CO_2, as well as sulfur as an important petrogenetic process in samples of this group.

The C, O, and S isotopic data are consistent with the interpretation of Santos and Clayton (1995) in that the APIP complexes were emplaced at shallower crustal levels than the Jacupiranga Complex. The lower lithostatic pressure at these shallower levels allowed a much greater diversity of petrogenetic processes to act in the evolution of the APIP carbonatite magmas, including fractional crystallization, liquid immiscibility, degassing, and interaction with hydrothermal and carbohydrothermal systems, often in recurring events (Barbosa *et al.* 2012, Brod *et al.* 2013, Cordeiro *et al.* 2010, Gomide *et al.* 2013).

ACKNOWLEDGMENTS

The authors are grateful to the Geochronology Laboratory at Universidade de Brasília and to CRTI at Universidade Federal de Goiás for access to analytical facilities and to the Brazilian agencies CNPq and CAPES for the financial support to this research.

REFERENCES

Almeida F.F.M. & Svisero D.P. 1991. Structural setting and tectonic control of Kimberlite and associated rocks of Brazil. *In*: Leonardos O.H., Meyer H.O.A., Gaspar J.C. (Eds). *5th International Kimberlite Conference*. CPRM, Araxá, Brazil, pp. 3-5.

Andrade S, Hypolito R, Ulbrich H.H.G.J., Silva M.L. 2002. Iron (II) oxide determination in rocks and minerals. *Chemical Geology*, **182**:85-89.

Araújo D.P. 1996. Produtos de Reacão de Carbonatitos Com Rochas Ultramáficas no Complexo Catalao I, Goiás: Implicações para o Metassomatismo Mantélico. MS Dissertation, Universidade de Brasília, Brasília.

Barbosa E.S.R. 2009. *Mineralogia e Petrologia do Complexo Carbonatítico-Foscorítico de Salitre, MG*. Ph.D. Thesis, Universidade de Brasília, Brasília, 434 pp.

Barbosa E.S.R., Brod J.A., Junqueira-Brod T.C., Dantas E.L., Cordeiro P.F.D., Gomide C.S. 2012. Bebedourite from its type area (Salitre I complex): A key petrogenetic series in the Late-Cretaceous Alto Paranaíba kamafugite-carbonatite-phoscorite association, Central Brazil. *Lithos*, **144**:56-72.

Brod J.A. 1999. *Petrology and geochemistry of the Tapira alkaline complex, Minas Gerais State, Brazil*. Ph.D. Thesis, University of Durham, Durham, UK, 486 pp.

Brod J.A., Gibson S.A., Thompson R.N., Junqueira-Brod T.C., Seer H.J., Moraes L.C., Boaventura G.R. 2000.The kamafugite-carbonatite association in the Alto Paranaíba igneous province, southeasthern Brazil.Revista Brasileira de *Geociências*, **30**:408-412.

Brod A.J., Junqueira-Brod T.C., Gaspar J.C., Gibson S.A., Thompsom R.N. 2003. Mineral-Chemistry fingerprints of liquid immiscibility and fractionation in the Tapira alkaline-carbonatite complex (Minas Gerais, Brazil). *In*: 8th International Kimberlite Conference, *Long Abstract*.

Brod J.A., Ribeiro C.C., Gaspar J.C., Junqueira-Brod T.C., Barbosa E.S.R., Riffel B.F., Silva J.F., Chaban N., Ferrari A.J.D. 2004. *Excursão 1*. Geologia e mineralizações dos complexos alcalino-carbonatíticos da Província Ígnea do Alto Paranaíba. *In*: Congresso Brasileiro de Geologia, XLII, Araxá, MG, pp. 1-29.

Brod J.A., Barbosa E.S.R., Junqueira-Brod T.C., Gaspar J.C., Diniz-Pinto H.S., Sgarbi P.B.A., Petrinovic I.A. 2005. The Late-Cretaceous Goiás Alkaline Province (GAP), Central Brazil. *In*: Piero Comin-Chiaramonti; Celso de Barros Gomes. (Eds). *Mesozoic and Cenozoic alkaline magmatism in the Brazilian Platform*. São Paulo: Edusp, p. 261-316.

Brod J.A., Junqueira-Brod T.C., Gaspar J.C., Petrinovic I.A., Valente S.d.C., Corval A. 2013.Decoupling of paired elements, crossover REE patterns, and mirrored spider diagrams: Fingerprinting liquid immiscibility in the Tapira alkaline–carbonatite complex, SE Brazil. *Journal of South American Earth Sciences*, **41**(0):41-56.

Brod J.A., Junqueira-Brod T.C., Gaspar J.C., Petrinovic I.A., Valente S.d.C., Corval A., 2013. Decoupling of paired elements, crossover REE patterns, and mirrored spider diagrams: Finger printing liquid immiscibility in the Tapira alkaline–carbonatite complex, SE Brazil. *Journal of South American Earth Sciences*, **41**(0):41-56.

Buhn B. & Rankin A.H. 1999. Composition of natural, volatile-rich Na-Ca-REE-Sr carbonatitic fluids trapped in fluid inclusions. *Geochimica Et Cosmochimica Acta*, **63**(22):3781-3797.

Carlson R.W., Araujo A.L.N., Junqueira-Brod T.C., Gaspar J.C., Brod J.A., Petrinovic I.A., Hollanda M., Pimentel M.M., Sichel S. 2007. Chemical and isotopic relationships between peridotite xenoliths and mafic-ultrapotassic rocks from Southern Brazil. *Chemical Geology*, **242**(3-4):415-434.

Chakhmouradian A.R., Mumin A.H., Demény A., Elliott B. 2008. Postorogenic carbonatites at Eden Lake, Trans-Hudson Orogen (northern Manitoba, Canada): Geological setting, mineralogy and geochemistry. *Lithos*, **103**(3-4):503-526.

Comin-Chiaramonti P., Gomes C.B., Ruberti E., Antonini P., Castorina F., Censi P. 2001. Mato Preto alcaline-carbonatite complex: geochemistry and isotope (O-C, Sr-Nd) constraints. *Geochimica Brasiliensis*, **15**(1/2):023-034.

Comin-Chiaramonti P., Gomes C.B., Censi P., Speziale S. 2005. Carbonatites from Southeastern Brazil: a model for the carbon and oxygen isotopic variations. *In*: Comin-Chiaramonti P. & Gomes C.B. (Eds.). *Mesozoic and Cenozoic alkaline magmatism in the Brazilian Platform*. EDUSP/FAPESP, São Paulo, p. 629-656.

Cordeiro P.F.O. 2009. *Petrologia e Metalogenia do depósito primário de nióbio do Complexo Carbonatítico-Foscorítico de Catalão I, GO*. MS Dissertation, Universidade de Brasília, Brasília, 202 p.

Cordeiro P.F.O., Brod J.A., Dantas E.L., Barbosa E.S.R. 2010. Mineral chemistry, isotope geochemistry and petrogenesis of niobium-rich rocks from the Catalão I carbonatite-phoscorite complex, Central Brazil. *Lithos*, **118**:223-237.

Cordeiro P.F.O., Brod J.A., Santos R.V., Dantas E.L., de Oliveira C.G., Barbosa E.S.R. 2011. Stable (C, O) andradiogenic (Sr, Nd) isotopes of carbonates as indicators of magmatic and post-magmatic processes of phoscorite-series rocks and carbonatites from Catalo I, central Brazil. *Contributions to Mineralogy and Petrology*, **161**(3):451-464.

Deines P. 1989. Stable isotope variations in carbonatites. *In*: Bel K. (Ed.). *Carbonatites: genesis and evolution*. Unwin Hyman, London, p. 301-359.

Druppel K., Wagner T., Boyce A.J. 2006. Evolution of sulfide mineralization in ferrocarbonatite, Swartbooisdrif, northwestern Namibia: Constraints from mineral compositions and sulfur isotopes. *Canadian Mineralogist*, **44**:877-894.

Gaspar J.C. & Wyllie P.J. 1982. Barium Phlogopite from the Jacupiranga Carbonatite, Brazil. *American Mineralogist*, **67**(9-10):997-1000.

Gaspar J.C. & Wyllie P.J. 1983. Magnetite in the carbonatites from the Jacupiranga complex, Brazil. *American Mineralogist*, **68**(1-2):195-213.

Gibson S.A., Thompson R.N., Leonardos O.H., Dickin A.P., Mitchell J.G., 1995. The Late Cretaceous Impact of the Trindade Mantle Plume - Evidence from Large-Volume, Mafic, Potassic Magmatism in Se Brazil. *Journal of Petrology*, **36**(1):189-229.

Gibson S.A., Thompson R.N., Weska R., Dickin A.P., Leonardos O.H. 1997. Late Cretaceous rift-related upwelling and melting of the Trindade starting mantle plume head beneath western Brazil. *Contributions to Mineralogy and Petrology*, **126**:303-314.

Gomes C.B., Ruberti E., Morbidelli L. 1990. Carbonatite complexes from Brazil: a review. *Journal of South American Earth Sciences*, **3**(1):51-63.

Gomes C.B. & Comin-Chiaramonti P. 2005. Some notes on the Alto Paranaíba Igneous Province. *In*: Comin-Chiaramonti P. & Gomes C.B. (eds). *Mesozoic to Cenozoic Alkaline Magmatism in the Brazilian Platform*. São Paulo, EDUSP, 750 p.

Gomide C.S., Brod J.A., Junqueira-Brod T.C., Buhn B., Santos R.V., Barbosa E.S.R., Cordeiro P.F.O., Palmieri M., Grasso C.B., Torres M.G. 2013. Sulfur isotopes from Brazilian alkaline carbonatite complexes. *Chemical Geology*, **341**:38-49.

Grasso C.B. 2010. *Petrologia do Complexo Alcalino-Carbonatítico de Serra Negra, MG*. MS Dissertation, Universidade de Brasília, Brasília, 209 p.

Hamilton D.L., Bedson P., Esson J. 1989. The behavior of trace elements in the evolution of carbonatites. *In*: Bell K. (ed). *Carbonatites: genesis and evolution*. London, Unwin Hyman, p. 405-427.

Huang Y.M., Hawkesworth C.J., Calsteren P.V., McDermott F. 1995. Geochemical characteristics and origin of the Jacupiranga carbonatites, Brazil. *Chemical Geology*, **119**:79-99.

Jones A.P., Wall F., Williams C.T. 1995. *Rare Earth Minerals: Chemistry, Origin and Ore Deposits*. Berlim, Springer-Verlag, 372 p.

Junqueira-Brod T.C., Gomide C.S., Brod J.A., Dardenne M.A., Palmieri M., Grasso C., Santos R.V. *In preparation*. Fluidisation processes and breccias formation in the Catalão I and Catalão II Complexes, Alto Paranaíba Igneous Province - APIP, Central Brazil – Evidence for magma fragmentation inside carbonatite magma chambers.

Le Bas M.J. & Handley C.D. 1979. Variation in apatite composition in ijolitic and carbonatitic igneous rocks. *Nature*, **279**:54-56.

Le Maitre R.W., Streckeisen A., Zanettin B., Le Bas M.J., Bonin B., Bateman P., Bellieni G., Dudek A., Efremova S., Keller J., Lameyre J., Sabine P.A., Schmid R., Sørensen H., Woolley A.R. 2002. Igneous *Rocks - A Classification and Glossary of Terms*. Recommendations of the International Union of Geological Sciences Subcommission on the Systematics of Igneous Rocks. Cambridge, Cambridge University Press, 256 p.

Leonardos O.H., Ulbrich M.N., Gaspar J.C. 1991. The Mata da Corda volcanic rocks. *In*: Leonardos O.H., Meyer H.O.A., Gaspar J.C. (eds). 5th International Kimberlite Conference. *Special Publication* 3/91. CPRM, Araxá, Brazil, p. 65-73.

Lloyd F.E. & Bailey D.K. 1991. The genesis of perovskite-bearing bebedourite and the problems posed by clinopyroxenite-carbonatite complexes, *In*: 5th International Kimberlite Conference, *Extended Abstracts*. CPRM, Araxá, Brazil, pp. 237-239.

Machado Junior D.L. 1992. Geologia do complexo alcalino-carbonatítico de Catalão II (GO). *In:* Congresso Brasileiro de Geologia, *Extended Abstracts Boletim*, São Paulo, Brazil, p. 94-95.

Mariano A.N. & Marchetto M. 1991. Serra Negra and Salitre - carbonatite alkaline igneous complex. *In*: Leonardos O.H., Meyer H.O.A., Gaspar J.C. (eds). 5th International Kimberlite Conference. *Special Publication* 3/91. CPRM, Araxá, Brazil, p. 75-79.

Mitchell R.H. & Krouse H.R. 1975. Sulphur isotope geochemistry of carbonatites. *Geochimica et Cosmochimica Acta*, **39**(11):1505-1513.

Morbidelli L., Gomes C.B., Beccaluva L., Brotzu P., Garbarino C., Riffel B.F., Ruberti E. & Traversa G. 1997. Parental magma characterization of Salitre cumulate rocks (Alto Paranaíba Alkaline Province, Brazil) as inferred from mineralogical, petrographic, and geochemical data. *International Geology Review*, **39**:723-743.

Nelson D.R., Chivas A.R., Chappel B.W., McCulloch M.T. 1988. Geochemical and isotopic systematics in carbonatites and implications for the evolution of ocean-island sources. *Geochimica et Cosmochimica Acta*, **52**:1-17.

Nikiforov A.V., Bolonin A.V., Pokrovsky B.G., Sugorakova A.M., Chugaev, A.V., Lykhin D.A. 2006. Isotope geochemistry (O, C, S, Sr) and Rb-Sr age of carbonatites in central Tuva. *Geology of Ore Deposits*, **48**(4):256-276.

Oliveira I.W.B., Sachs L.L.B., Silva V.A., Batista I.H. 2004. Folha SE. 23-Belo Horizonte. *In*: Schobbenhaus C., Gonçalves J.H., Santos J.O.S., Abram M.B., Leão Neto R., Matos G.M.M., Vidotti R.M., Ramos M.A.B., Jesus J.D.A. (ed.). *Carta Geológica do Brasil ao Milionésimo: Sistema de Informações Geográficas - SIG e 46 folhas na escala 1 : 1.000.000*. Brasília, CPRM. 41 CD-ROM Pack.

Palmieri M. 2011. *Modelo Geológico e Avaliação de Recursos Minerais do Depósito de Nióbio Morro do Padre, Complexo alcalino-carbonatítico Catalão II, GO.* MS, Universidade de Brasília, Brasília, 130 p.

Ray J.S. & Ramesh R. 2000. Rayleigh fractionation of stable isotopes from a multicomponent source. *Geochimica et Cosmochimica Acta*, **64**:299-306.

Ribeiro C.C. 2008. *Geologia, geometalurgia, controles e gênese dos depósitos de fósforo, terras raras e titânio do Complexo Carbonatítico de Catalão I, GO.* Ph. D. Thesis, Universidade de Brasília, Brasília, 473 p.

Ribeiro C.C., Brod J.A., Junqueira-Brod T.C., Gaspar J.C., Petrinovic I.A., 2005. Mineralogical and field aspects of magma fragmentation deposits in a carbonate-phosphate magma chamber: evidence from the Catalao I complex, Brazil. *Journal of South American Earth Sciences*, **18**(3-4):355-369.

Ribeiro C.C., Brod J.A., Junqueira-Brod T.C., Gaspar J.C., Palmieri M., Cordeiro P.F.O., Torres M.G., Grasso C.B., Barbosa E.S.R., Barbosa P.A.R., Ferrari A.J.D., Gomide C.S. 2014. Potencial e controles metalogenéticos de ETR, Ti e Nb em províncias alcalino-carbonatíticas brasileiras. *Metalogenia das Províncias Tectônicas do Brasil*. CPRM, Brasília, p. 559-589.

Ruberti E., Gomes C.B., Comin-Chiaramonti P. 2005. The alkaline magmatism from the Ponta Grossa Arch. *In*: Comin-Chiaramonti P. & Gomes C.B. (eds). *Mesozoic to Cenozoic Alkaline Magmatism in the Brazilian Platform*. São Paulo, Edusp/Fapesp, 750 p.

Sahama T.G. 1974. Potassium-rich alkaline rocks. *In*: Sørensen H. (ed). *The Alkaline Rocks*. New York, Wiley, p. 96-109.

Santos R.V. & Clayton R.N. 1995. Variations of oxygen and carbon isotopes in carbonatites: a study of Brazilian alkaline complexes. *Geochimica Et Cosmochimica Acta*, **59**(7):1339-1352.

Seer H.J. 1999. *Evolução Tectônica dos Grupos Araxá e Ibiá na Sinforma de Araxá-MG*. Ph. D. Thesis,Universidade de Brasília, Brasília, 267 p.

Seer H.J. & Moraes L.C. 1988. Estudo petrográfico das rochas ígneas alcalinas da região de Lagoa Formosa, MG. *Revista Brasileira de Geociências*, **18**:134-140.

Spotl C. & Vennemann T.W. 2003. Continuous-flow isotope ratio mass spectrometric analysis of carbonate minerals. *Rapid Communications in Mass Spectrometry*, **17**:1004-1006.

Stoppa F. & Cundari A. 1995. A new Italian carbonatite occurrence at Cupaello (Rieti) and its genetic significance. *Contributions to Mineralogy and Petrology*, **122**(3):275-288.

Stoppa F. & Wooley A.R. 1997. The Italian carbonatites: Field occurrence, petrology and regional significance. *Mineralogy and Petrology*, **59**(1-2):43-67.

Taylor H.P., Frechen J., Degens E.T. 1967. Oxygen and carbon isotope studies of carbonatites from the Laacher See district, West Germany, and the Alno district, Sweden. *Geochimica et Cosmochimica Acta*, **31**:407-430.

Thompson N. 1982. Magmatism of the British Tertiary Volcanic Province (Carnegie Review Article). *Scottish Journal of Geology*, **18**:49-107.

Traversa G., Gomes C.B., Brotzu P., Buraglini N., Morbidelli L., Principato M.S., Ronca S., Ruberti E. 2001. Petrography and mineral chemistry of carbonatites and mica-rich rocks from the Araxa complex (Alto Paranaíba Province, Brazil). *Anais da Academia Brasileira de Ciencias*, **73**(1):71-98.

Ulbrich H.H.G.J. & Gomes C.B. 1981. Alkaline rocks from continental Brazil. Earth Science Reviews, **17**:135-154.

Veksler I.V., Petibon C., Jenner G. A., Dorfman A.M., Dingwell D.B. 1998. Trace element partitioning in immiscible silicate-carbonate liquid systems: An initial experimental study using a centrifuge autoclave. *Journal of Petrology*, **39**(11-12):2095-2104.

Veksler I.K., Dorfman A.M., Dulski P., Kamenetsky V.S., Danyushevsky L.V., Jeffries T., Dingwell D.B. 2012. Partitioning of elements between silicate melt and immiscible fluoride, chloride, carbonate, phosphate and sulfate melts, with implications to the origin of natrocarbonatite. *Geochimica et Cosmochimica Acta*, **79**:20-40.

Whitney D.L. & Evans B.W. 2010. Abbreviations for names of rock-forming minerals. *American Mineralogist*, **95**:185-187.

Woolley A.R. & Kjarsgaard B.A. 2008. *Carbonatite Occurrences of the World:* Map and Database, Geological Survey of Canada. 1 CD-ROM + 1 map.

Woolley A.R. & Kempe D.R.C. 1989. Carbonatites: nomenclature, average chemical compositions, and element distribution. *In*: Bell K. (ed.). *Carbonatites: genesis and evolution*. London, Unwin Hyman, p. 1-14.

Yegorov L.S. 1993. Phoscorites of the Maymecha-Kotuy ijolite-carbonatite association. *International Geology Reviews*, **35**:346-358.

Xie Y., Hou Z., Yin S., Dominy S.C., Xu J., Tian S., Xu W. 2009. Continuous carbonatitic melt-fluidexolution of a REE mineralization system: Evidence from inclusion in the Maoniuping REE Deposit, Western Sichuan, China. *Ore Geology Reviews*, **36**:90-105.

Zaitsev A.N., Wall F., Le Bas M.J. 1998. REE-Sr-Ba minerals from the Khibina carbonatites, Kola peninsula, Russia: their mineralogy, paragenesis and evolution. *Mineralogical Magazine*, **62**(2):225-250.

Available at www.sbgeo.org.br

Appendix 1 – Supplementary data – Major Elements
Aditional data were published by Brod (1999), Barbosa (2009), Cordeiro (2009), Grasso (2010) and Palmieri (2011).

Sample	C2AA165907	SLE360	TPTAPS	J15052C	J15053E	JC1	JC3B	J15053D	J1605	J17052B	JC3
Unit	C1	C1	C1	C1a	C1a	C1a	C1a	C1b	C1b	C1b	C1b
Complex	Catalão II	Salitre	Tapira	Jacupiranga	Jacupiranga	Jacupiranga	Jacupiranga	Jacupiranga	Jacupiranga	Jacupiranga	Jacupiranga
Province	APIP	APIP	APIP	Ponta Grossa	Ponta Grossa	Ponta Grossa	Ponta Grossa	Ponta Grossa	Ponta Grossa	Ponta Grossa	Ponta Grossa
SiO_2	8.93	0.06	1.16	0.29	0.80	2.49	1.70	0.06	0.81	0.21	0.17
TiO_2	0.44	0.01	0.10	0.00	0.06	0.13	0.74	0.00	0.01	0.02	0.04
Al_2O_3	0.20	0.00	0.06	0.00	0.27	0.16	0.18	0.00	0.02	0.04	0.03
$Fe_2O_{3(T)}$	10.50	1.62	4.48	0.43	9.51	3.97	2.82	1.96	1.52	1.88	2.04
MnO	0.25	0.12	0.11	0.12	0.15	0.12	0.13	0.12	0.13	0.13	0.13
MgO	2.56	0.79	2.44	6.05	3.96	4.78	4.61	3.92	5.87	4.36	3.67
CaO	39.90	53.84	50.78	48.53	46.27	47.59	48.38	52.12	49.07	50.17	50.74
Na_2O	0.82	0.17	0.09	0.04	0.05	0.09	0.07	0.02	0.03	0.03	0.04
K_2O	0.63	0.11	0.11	0.00	0.03	0.11	0.15	0.00	0.00	0.02	0.03
P_2O_5	1.49	0.01	4.25	11.30	11.85	19.74	15.80	0.06	4.94	5.16	3.51
BaO	0.47	0.35	0.22	0.06	0.07	0.14	0.10	0.08	0.07	0.09	0.36
SrO	1.65	2.08	1.58	0.66	0.62	0.48	0.64	0.69	0.71	0.72	0.78
LOI	31.70	40.70	34.00	32.30	26.10	19.60	24.40	40.80	36.60	37.00	38.30
Nb_2O_5	0.04	0.00	0.14	0.00	0.00	0.01	0.02	0.00	0.00	0.00	0.00
REE_2O_3	0.30	0.17	0.27	0.09	0.11	0.15	0.13	0.05	0.07	0.08	0.07
Total	99.92	100.01	99.81	99.89	99.93	99.87	99.88	99.89	99.87	99.90	99.92
CO_2	34.59	44.38	37.52	34.01	28.99	20.63	28.18	45.15	38.00	39.98	41.44
TotS	0.75	0.62	0.63	0.13	0.28	0.05	0.62	0.56	0.38	0.14	0.49

Sample	JC4	JCCG01	JCCG02	JCL250	C1CB02	J080DIQUE	J140N3B	AXC85D	SL109C	AXC83E	AXC83H	C1L15250
Unit	C1b	C1b	C1b	C1b	C2	C2	C2	C4	C4	C5	C5	C5
Complex	Jacupiranga	Jacupiranga	Jacupiranga	Jacupiranga	Catalão I	Jacupiranga	Jacupiranga	Araxá	Salitre	Araxá	Araxá	Catalão I
Province	Ponta Grossa	Ponta Grossa	Ponta Grossa	Ponta Grossa	APIP	Ponta Grossa	Ponta Grossa	APIP	APIP	APIP	APIP	APIP
SiO_2	0.57	0.17	0.13	0.34	0.23	0.41	0.24	2.64	1.34	0.49	0.22	1.75
TiO_2	0.01	0.00	0.00	0.00	0.01	0.00	0.00	0.14	0.38	0.04	0.25	0.08
Al_2O_3	0.10	0.00	0.01	0.04	0.00	0.05	0.09	0.12	0.09	0.01	0.00	0.08
$Fe_2O_{3(T)}$	4.44	38.78	0.23	5.66	6.00	4.46	0.62	5.75	2.61	5.26	2.93	9.88
MnO	0.12	0.07	0.14	0.12	0.36	0.22	0.13	0.69	0.56	0.37	0.29	0.28
MgO	3.82	0.88	3.82	3.24	19.67	17.36	14.74	15.62	14.65	16.80	16.33	14.60
CaO	47.59	30.38	50.73	50.15	30.29	33.39	37.91	24.57	28.73	20.09	20.05	23.23
Na_2O	0.05	0.02	0.02	0.03	0.11	0.06	0.05	0.24	0.17	0.16	0.19	0.05

Continue...

Appendix 1 – Continuation.

Sample	JC4	JCCG01	JCCG02	JCL250	C1CB02	J080DIQUE	J140N3B	AXC85D	SL109C	AXC83E	AXC83H	C1L15250
Unit	C1b	C1b	C1b	C1b	C2	C2	C2	C4	C4	C5	C5	C5
Complex	Jacupiranga	Jacupiranga	Jacupiranga	Jacupiranga	Catalão I	Jacupiranga	Jacupiranga	Araxá	Salitre	Araxá	Araxá	Catalão I
Province	Ponta Grossa	Ponta Grossa	Ponta Grossa	Ponta Grossa	APIP	Ponta Grossa	Ponta Grossa	APIP	APIP	APIP	APIP	APIP
K_2O	0.06	0.00	0.00	0.03	0.14	0.03	0.05	0.15	0.22	0.12	0.09	0.31
P_2O_5	8.24	0.00	0.39	5.68	0.10	3.46	13.88	6.26	6.69	0.71	0.08	4.34
BaO	0.08	0.07	0.13	0.09	0.18	0.04	0.03	3.88	5.59	11.12	13.72	8.51
SrO	0.60	0.41	0.86	0.66	1.27	0.54	0.42	3.87	3.13	3.12	3.20	2.24
LOI	34.20	3.40	43.40	33.80	41.20	39.50	31.50	33.00	32.20	36.10	39.10	31.20
Nb_2O_5	0.00	0.00	0.00	0.01	0.00	0.07	0.00	0.04	0.01	0.22	0.03	0.04
REE_2O_3	0.06	0.04	0.06	0.07	0.09	0.05	0.06	2.50	2.13	0.31	0.20	0.21
Total	99.95	74.22	99.92	99.91	99.64	99.64	99.73	99.50	101.44	98.79	99.00	100.48
CO_2	36.86	25.72	42.51	35.95	40.05	42.18	33.05	35.73	32.32	36.75	36.50	30.78
TotS	0.31	16.73		0.60	2.42	1.92		1.15	1.38	1.55	0.93	2.13

Sample	C2AA165907	SLE360	TPTAPS	J15052C	J15053E	JC1	JC3B
Unit	C1	C1	C1	C1a	C1a	C1a	C1a
Complex	Catalão II	Salitre	Tapira	Jacupiranga	Jacupiranga	Jacupiranga	Jacupiranga
Province	APIP	APIP	APIP	Ponta Grossa	Ponta Grossa	Ponta Grossa	Ponta Grossa
Ba	4174	3178	1971	575	646	1270	907
Rb	24.6	1.6	2.3	0.1	0.9	2.9	4.3
Sr	13981	17560	13364	5592.3	5259.5	4067	5450.6
Cs	0.3					0.1	
Ga	4.5		0.9		1.7	1.4	0.5
Ta	31.6	0.1	104.9	0.6	12.5	6.7	11.5
Nb	310.3	14.2	996.8	0.5	29.3	42	152.2
Hf	4		3.6	1.7	7.8	5.2	0.1
Zr	312.6	3.5	112.2	132.9	554.8	2321.4	7.3
Y	93.5	53.9	74.2	46.3	53	50.7	55.5
Th	158.2	10.5	437.2	1.5	2	12.7	7.2
U	32.4	0.8	305.1		0.3	2.3	0.8
Ni		3.2		0.2		0.2	46.5
V	106		57		93	88	34
Cu	22	26.8	7.6	6.8	4.8	8.3	133.3
Pb	27.6	6.4	4.3	6.1	6.1	3.5	5.2
Zn	58	3	19	1	32	19	7
Sc	5	4	14	8	20	34	12

Continue...

Appendix 1 – Continuation.

Sample	C2AA165907	SLE360	TPTAPS	J15052C	J15053E	JC1	JC3B
Unit	C1	C1	C1	C1a	C1a	C1a	C1a
Complex	Catalão II	Salitre	Tapira	Jacupiranga	Jacupiranga	Jacupiranga	Jacupiranga
Province	APIP	APIP	APIP	Ponta Grossa	Ponta Grossa	Ponta Grossa	Ponta Grossa
Co	13.9	10.4	33.7	9.4	32.6	9.2	40.2
La	643.4	373.2	471.8	141.8	165.9	223.1	200.6
Ce	1200.4	700.6	1103.8	331.3	394.4	550.8	495.3
Pr	121.28	68.81	122.34	40.88	48.93	68.9	62.59
Nd	422.5	230.9	477.1	174.7	204.5	289.7	265.9
Sm	46.71	26.2	62.48	29.57	35.27	46.23	44.06
Eu	12.1	7.28	15.87	8.5	9.83	12.76	12.32
Gd	35.88	21.16	45.54	23.57	27.56	36.54	36.4
Tb	4.66	2.27	4.28	2.76	3.25	3.68	3.75
Dy	21.87	10.04	18.01	12.1	14.1	15.62	16.28
Ho	3.35	1.66	2.62	1.72	2.03	2.01	2.25
Er	7.49	4.02	5.41	3.5	4.31	3.93	4.43
Tm	0.93	0.6	0.67	0.42	0.48	0.39	0.49
Yb	5.29	3.48	3.73	2.27	2.56	2.3	2.89
Lu	0.72	0.53	0.49	0.29	0.31	0.26	0.35

Sample	J15053D	J1605	J17052B	JC3	JC4	JCCG01	JCCG02	JCL250
Unit	C1b	C1b	C1b	C1b	C1b	C1b	C1b	C1b
Complex	Jacupiranga	Jacupiranga	Jacupiranga	Jacupiranga	Jacupiranga	Jacupiranga	Jacupiranga	Jacupiranga
Province	Ponta Grossa	Ponta Grossa	Ponta Grossa	Ponta Grossa	Ponta Grossa	Ponta Grossa	Ponta Grossa	Ponta Grossa
Ba	760	621	777	3206	708	637	1169	764
Rb	0.1		0.4	0.9	1.2		0.3	
Sr	5872.2	6044.4	6062.2	6613	5043.1	3473.1	7267.1	5562.2
Cs								
Ga					0.7	0.7		1
Ta	0.3	1.1	1.6	0.3	6.2		0.5	2.1
Nb	6.6	3.1	4.1	3.9	12.3	8.7	11.9	39.3
Hf		1.6	0.2	0.1	1.8			0.4
Zr	8.6	109.7	4.1	6.8	107.5	6	1.1	27.1
Y	36.7	39.5	42.7	44.1	50.1	21.4	42.5	38.5
Th	0.4	0.9	1.8	0.7	1.8		0.7	4.3
U					0.2			
Ni		1.5		4.8		102	0.2	
V			12	19	39			32

Continue...

Appendix 1 – Continuation.

Sample	J15053D	J1605	J17052B	JC3	JC4	JCCG01	JCCG02	JCL250
Unit	C1b	C1b	C1b	C1b	C1b	C1b	C1b	C1b
Complex	Jacupiranga	Jacupiranga	Jacupiranga	Jacupiranga	Jacupiranga	Jacupiranga	Jacupiranga	Jacupiranga
Province	Ponta Grossa	Ponta Grossa	Ponta Grossa	Ponta Grossa	Ponta Grossa	Ponta Grossa	Ponta Grossa	Ponta Grossa
Cu	2.1	20.2	9.8	27.7	0.8	361.9	43.1	34.6
Pb	4.6	5.7	5.4	8.1	12.7	10.8	8.1	6.5
Zn	2	6	6	6	13	20	1	14
Sc	10	11	12	13	14	13	13	15
Co	44.3	23.8	14.2	31.1	38.3	394.2	1.9	57.2
La	95.7	111.9	126.6	125.2	87.7	67.7	112.3	120.7
Ce	189.9	248.3	280	280.7	201.8	144.4	234.2	244.5
Pr	22.98	29.72	33.31	32.03	24.5	16.35	26.81	29.48
Nd	94.7	125.3	133.6	125.2	103	61.5	105.8	118.7
Sm	15.62	21.26	23.51	21.99	19.48	10.55	17.64	19.72
Eu	4.67	6.16	6.7	6.48	6.01	3.03	5.4	5.95
Gd	12.37	16.77	18.86	18.92	18.67	8.1	15.48	15.44
Tb	1.69	2.12	2.31	2.25	2.34	1.06	1.94	2.07
Dy	8.34	9.79	10.26	10.53	11.03	4.75	9.28	9.11
Ho	1.2	1.49	1.55	1.61	1.92	0.73	1.58	1.37
Er	2.86	3.36	3.38	3.72	4.41	1.62	3.39	3.12
Tm	0.39	0.41	0.41	0.44	0.54	0.21	0.43	0.37
Yb	2.25	2.14	2.46	2.54	3.13	1.08	2.46	1.97
Lu	0.28	0.28	0.31	0.34	0.42	0.14	0.36	0.28

Sample	C1CB02	J080DIQUE	J140N3B	AXC85D	SL109C	AXC83E	AXC83H	C1L15250
Unit	C2	C2	C2	C4	C4	C5	C5	C5
Complex	Catalão I	Jacupiranga	Jacupiranga	Araxa	Salitre	Araxa	Araxa	CatalaoI
Province	APIP	Ponta Grossa	Ponta Grossa	APIP	APIP	APIP	APIP	APIP
Ba	1573	340	231	34714	50067	99597	122884	76220
Rb	1.7	0.8	1.1	4.7	5.1	4.4	1.8	19.5
Sr	10723	4553.3	3587.7	32731	26480	26342	27028	18975
Cs								0.3
Ga	0.8	0.8	0.6					1.4
Ta		20.6	1	3.7	0.5	6.1	5.8	73.5
Nb	20.3	489.5	2.2	307.9	88.9	1563.4	200.9	305.7
Hf	1	0.5	1	5	3	1.8	1.6	4.5
Zr	30.4	18.2	66	217.2	97.3	11.8	13.1	170.8
Y	10.7	27.2	38.8	224.4	95	32.5	46.4	24.1

Continue...

Appendix 1 – Continuation.

Sample	C1CB02	J080DIQUE	J140N3B	AXC85D	SL109C	AXC83E	AXC83H	C1L15250
Unit	C2	C2	C2	C4	C4	C5	C5	C5
Complex	Catalão I	Jacupiranga	Jacupiranga	Araxa	Salitre	Araxa	Araxa	CatalaoI
Province	APIP	Ponta Grossa	Ponta Grossa	APIP	APIP	APIP	APIP	APIP
Th	12.1	33	1.9	330.5	57.8	108.6	148.7	18.3
U	2.4	0.6	0.1	3.8	2.5	2	2	20.2
Ni	14.4			55.2	4.1	5		4
V		9		50	18	15	19	57
Cu	335.4	4.7	0.5	1.5	88.1	16.6	1.7	190.4
Pb	3.2	21.1	2.5	1029.5	193.4	32	15.7	3.6
Zn	10	11	3	392	261	105	22	22
Sc	13	14	7	43	13	20	20	14
Co	102	22.2	1.8	21.7	9.2	45.2	21.2	145.9
La	153.7	83.1	81.2	4930.8	6354.1	719.1	535.4	397.9
Ce	375.2	174.9	196.8	11000.7	8541.2	1277.4	793.7	860.4
Pr	46.02	22.52	26.02	1053.1	700.1	124.93	73.31	95.72
Nd	181.6	96.3	110.4	3552.2	2203.9	412.2	236.5	362.7
Sm	25.75	17.08	21	388.4	200.85	46.37	35.94	47.95
Eu	6.31	5.17	6.23	86.13	44.82	9.13	8.14	11.48
Gd	11.36	13.61	18.09	264.68	81.99	37.38	36.15	34.05
Tb	1.08	1.8	2.3	16.86	8.74	3.6	4.19	2.6
Dy	3.34	7.86	10.21	66.04	30.37	12.5	15.65	8.26
Ho	0.31	1.08	1.54	7.32	2.98	1.35	1.78	0.92
Er	0.58	2.3	3.21	12.64	6.66	2.22	2.83	1.26
Tm	0.08	0.25	0.36	1.66	0.76	0.22	0.29	0.15
Yb	0.45	1.26	1.83	9.86	4.27	1.39	1.63	0.89
Lu	0.06	0.15	0.21	1.02	0.45	0.18	0.2	0.1

Supplementary data – Trace Elements and Rare Earth Elements
APIP: Alto Paranaíba Igneous Province.
Aditional data were published by Brod (1999), Barbosa (2009), Cordeiro (2009), Grasso (2010) and Palmieri (2011). APIP: Alto Paranaíba Igneous Province.